buildings

MDPI

Review

Towards Performance-Based Design of Masonry Buildings: Literature Review

Bowen Zeng and Yong Li *

Department of Civil and Environmental Engineering, University of Alberta, 9211-116 Street, Edmonton, AB T6G 1H9, Canada; bzeng1@ualberta.ca
* Correspondence: yong9@ualberta.ca

Abstract: Masonry is among the most widely used construction materials around the world. Contemporary masonry buildings are primarily designed to comply with prescriptive building code regulations. In recent decades, performance-based design (PBD) has gained increasing attention and achieved significant success in critical structures or infrastructure systems. Instead of being the first mover, the masonry research and practice community can be a faster follower in response to the design paradigm shift towards PBD for masonry buildings. A reliable performance assessment of masonry buildings is of paramount importance in the PBD framework. To facilitate this, this paper presents an up-to-date comprehensive literature review of experimental and analytical studies with emphasis on their contributions to advancement towards performance assessment of masonry buildings. This review categorized available works into two sub-topics: (1) traditional unreinforced masonry and (2) modern reinforced masonry. In each sub-topic, studies focusing on the structural behaviors of masonry at the component-level (i.e., masonry wall) are discussed first, followed by the building system-level-related studies. Through this literature review, the current state of the art and remaining research gaps are identified to provide guidance for future research needs and to pave the way for implementing PBD in the masonry industry.

Keywords: performance-based design; masonry buildings; seismic behavior; experimental tests; analytical models; hysteretic behavior

Citation: Zeng, B.; Li, Y. Towards Performance-Based Design of Masonry Buildings: Literature Review. *Buildings* **2023**, *13*, 1534. https://doi.org/10.3390/buildings13061534

Academic Editors: Elena Ferretti and Maria Teresa De Risi

Received: 4 May 2023
Revised: 30 May 2023
Accepted: 13 June 2023
Published: 15 June 2023

1. Introduction

Buildings in seismic-prone areas face increasing challenges in both the structural design and performance assessment stages in the context of resilient and sustainable constructions. Buildings' vulnerability to strong seismic events, as evidenced by past earthquakes, has raised concerns in design and retrofitting. The advent of more stringent building codes compounds this problem because they require major changes in the way that structures are designed and built. In modern building constructions, structural resilience is a desirable feature characterized by a lower probability of damage or failure, reduced damage under extreme events, and fast recovery (e.g., downtime, easy repair, and replacement). As revealed by recent natural hazard events, such as the 2011 Christchurch earthquake [1,2], building damage can remarkably affect the post-event recovery, resulting in considerable economic costs and downtime. To address this issue, modern structural design guidelines are shifting towards performance-based design, which is promoted as the future of design against natural hazards and is already practiced as an alternative to traditional prescriptive code-based design, particularly for challenging tasks such as the design of critical structures and infrastructure systems, such as tall buildings [3], highway bridges [4,5], railway bridges [6], nuclear power plants [7]. Masonry, as a relatively inexpensive, durable, and readily accessible construction material, has applications as structural walls (e.g., shear walls, load-bearing walls) in conventional low- or mid-rise buildings, due to its high strength, tested durability, inherent fire resistance, and energy efficiency. Masonry walls have been widely used as the predominant structural components in residential,

commercial, and school buildings. However, compared to modern concrete, steel, and timber buildings, masonry buildings have been put in a disadvantageous position partly due to its outdated design methods. On the other hand, masonry walls have traditionally been used as infill walls to separate inner and outer space by closing the perimeter of a frame building as enclosures. Thus, it is common to find applications of masonry infill walls with reinforced concrete frames, steel frames, and timber frames, where they are typically not considered as structural components during the structural design and performance evaluation process. However, the use of masonry infill walls has declined in recent years because of their alternatives, such as light steel/timber framed infill walls in both steel and timber framed buildings.

Currently, masonry buildings are primarily designed to adhere to prescriptive building code regulations, which establish specific construction practices to ensure performance satisfaction at the life-safety and/or collapse-prevention level. In North America, several design codes are available for the design of masonry structures, including the Canadian Standard Association (CSA) S304-14 "Design of Masonry Structures" [8], The Masonry Society (TMS) 402 "Building Code Requirements and Specification for Masonry Structures" [9], and the "National Building Codes of Canada" (NBCC) [10]. These prescriptive codes generally provide guidelines on the material properties, detailing requirements, minimum reinforcements, allowable stresses, and other considerations. Since it is impractical to have rules that apply to each combination of occupancy, building configuration, and building material used, code requirements are generally developed to apply to a wide range of buildings, with the final objective being to simplify the design process and provide a consistent approach and procedure. As a result, the applicability and appropriateness of such rules to any single building vary significantly. In fact, it has also been widely recognized that buildings with higher perceived risk or importance (e.g., emergency facilities, hospitals, and schools) should perform better than buildings that are categorized as "normal" buildings according to the building classifications based on their relative importance [11]. Code design requirements for such buildings are more stringent to ensure high reliability for the life safety of occupants or, for critical buildings, to provide for building functionality after natural hazards (e.g., earthquakes). However, the adequacy of current code provisions for these purposes is generally not ensured through explicit performance verification.

Experimental and analytical research efforts have played a vital role in shaping the development of masonry building design and construction, contributing to the evolution of design regulations, and fostering a deeper understanding of the complex behaviors of masonry buildings. Over the past few decades, a scientific basis has been overlaid on what originated as a purely heuristic code development process, enabling the incorporation of research findings. However, design codes for masonry buildings in the current versions do not still lead to rational design outcomes, with many being overly conservative. For instance, Hwang et al. [12] found that the design equations specified by the New Zealand Society for Earthquake Engineering (NZSEE) and Federal Emergency Management Agency (FEMA) 273 [13] result in quite conservative evaluations of the in-plane resistance of unreinforced masonry (URM) walls with a large deviation, particularly when the precompression stress is less than 0.5 MPa. Haach et al. [14] compiled an experimental database and evaluated the performance of the Eurocode 6 [15], finding that both design code models yielded overly conservative results with a large scatter. Izquierdo [16] investigated the performance of design codes CSA S304-14 [8] and TMS 402 [9] for the in-plane strength of partially grouted reinforced masonry (RM) walls, concluding that these two design codes were conservative, involving high errors and inconsistencies.

Given the limitations and conservatism of current masonry design codes, PBD offers an effective alternative that addresses these shortcomings and provides a more rational and objective framework for masonry buildings. Instead of being the first mover, the masonry research and practice community can be a faster follower in response to the design paradigm shift towards PBD for masonry buildings. However, such research-based studies or practice-oriented applications are rare. Abrams [17] explored the PBD concepts

introduced in FEMA Guidelines for Seismic Rehabilitation [13] in terms of the seismic assessment and rehabilitation of URM buildings, suggesting that the design of URM buildings should follow both displacement-based and force-based criteria. The primary reason is that some failure mechanisms (e.g., rocking and sliding) of URM components and buildings are inherently displacement-controlled actions. In such cases peak strengths can be resisted as large nonlinear deformations are imposed during seismic actions, creating a need to depict not only the strength but also its stiffness and deformation capacity at various performance states. It was also suggested in [17] that analytical techniques for estimating the lateral force–deflection relation should be examined, and more refined analytical models and tools may need to be developed. Heerema et al. [18] pointed out that there are several fundamental drawbacks, pertaining to inherently erroneous assumptions of the independence of strength and stiffness, in the widely used force-based seismic design approach.

It can be seen that within the context of PBD, reliable performance assessment of masonry buildings (e.g., strength, stiffness, ductility, crack pattern, and energy dissipation capacity) is essential, which can be assessed experimentally or analytically. For masonry buildings, this is much more challenging compared to other structural systems (e.g., steel, concrete buildings) due to the complexity of masonry with inherent heterogeneity. Some recent literature reviews are available for this research topic [19–23]. Celano et al. [19] performed a review of the existing design formulations for the in-plane strength of URM walls and then compared the design-code predictions with experimentally observed values. Shabani et al. [20] reviewed the simplified analytical methods for the seismic vulnerability assessment of URM buildings. D'Altri et al. [21] conducted a literature review about the existing modeling strategies for the analysis of URM structures and further proposed a classification strategy. Cattari et al. [22] discussed the advantages, limitations, and open problems related to the use of different modeling techniques for URM buildings under seismic loadings, with particular interest in nonlinear static analysis. El-Dakhakhni and Ashour [23] presented a literature survey on experimental and analytical works pertaining to the seismic response of RM shear walls and buildings. It can be seen that these review works mainly focused on the strength-based characterization of conventional URM walls and buildings or on general computational and analytical strategies for masonry structures, and very limited attention has been aligning available studies with the performance assessment of RM walls and buildings.

As such, this paper presents a literature review on relevant experimental and analytical/numerical works of masonry walls or buildings, which can potentially facilitate PBD assessment and design of masonry buildings, as well as the current literature status related to PBD design and assessment of both conventional URM and modern RM buildings. This literature review aims to identify the research needs to support the full implementation of next-generation PBD for masonry buildings, in which masonry walls are used as the primary structural components (i.e., masonry infill walls are excluded). In response to the research required to support full implementation of performance-based seismic design [11], particular interest lies in the experimental and numerical studies that facilitate the understanding and/or prediction of the structural performance of masonry wall components and buildings. In the literature identification procedure, an initial search was conducted by using the specific keyword "masonry wall(s)/building(s)" in various databases, such as the Web of Science and Google Scholar. Subsequently, additional filtering was added by using a set of related keywords, such as "unreinforced/reinforced", "experimental/numerical/analytical", "simplified/detailed micro models or macro models", "seismic behavior/performance assessment/evaluation", and "fragility analysis", to identify the most relevant and representative works. Furthermore, in order to provide the general context of performance-based seismic design, some classical and representative works are also included. This leads to a total of 252 publications reviewed thoroughly. With that, the remaining part of this review paper is organized as follows: Section 2 briefly describes the history and development of PBD. Section 3 reviews the experimental works

which can contribute to the performance assessment of masonry shear walls and masonry buildings, and relevant numerical studies are discussed in Section 4. Section 5 discusses the fragility and performance assessment of masonry walls and buildings based on the available experimental and numerical works. Finally, Section 6 presents the concluding remarks.

2. History and Development of Performance-Based Design

Traditional prescriptive-based designs mainly rely on predetermined rules and minimum requirements, which often result in conservative and inefficient designs without the flexibility to adapt to varying structural systems and loading scenarios. PBD has emerged as a transformative approach, addressing these limitations while offering a more rational, objective, and quantitative design framework.

PBD is founded on the premise that structural systems must fulfill specific performance objectives with explicit checks or verifications. In PBD, well-defined performance expectations are established for the finalized design, with minimal prescriptive processes. Consequently, PBD reverses the conventional structural design process by setting the end goal as the starting point. Engineers then engage creativity and leverage scientific principles of structural and material mechanics, free from unnecessary and often counterproductive prescriptive code requirements, to identify optimal solutions to satisfy multiple and competing objectives. The implementation of PBD design is completed by demonstrating compliance with performance expectations through analysis, simulation, testing, or a combination of these methods. The basic procedure of PBD can be illustrated in Figure 1, with a formal and clear definition of quantitative performance objectives, the development of a preliminary design, and an assessment to determine if the pre-set performance objectives were satisfied or not.

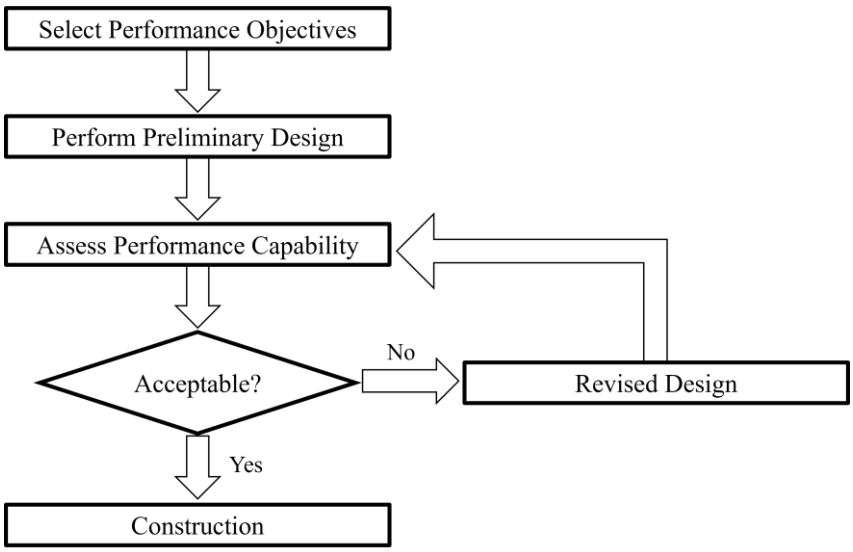

Figure 1. Performance-based design process.

Driven by a series of frequent but moderate-magnitude earthquakes in California during the mid-1980s, the first generation of PBD was proposed in the National Earthquake Hazards Reduction (NEHRP) Guidelines for the Seismic Rehabilitation of Existing Buildings FEMA 273, published in 1997 [13]. This document focused on the retrofit of existing buildings and contained a range of formal performance objectives that corresponded to specified levels of seismic shaking. The performance levels, intended for different stakeholders, were generalized into four categories: operational, immediate occupancy, life safety, and collapse prevention. Concurrently, the Structural Engineers Association of California (SEAOC) developed a more generalized PBD process, widely known as Vision 2000 [24], with similar performance objectives defined in FEMA 273.

FEMA 273 was later refined as FEMA 356, incorporating the new building design guidelines. FEMA 356 was then republished by the American Society of Civil Engineers as the ASCE/SEI 41-06 Standard. The evolution of FEMA series guidelines marked significant advancements in PBD. For instance, FEMA 440 was published in Year 2004 to provide a more reliable performance assessment approach for buildings. After several iterations, the contemporary design guideline generated through the NEHRP programs is FEMA P-2082 [25].

The advancements of PBD in structural engineering can be attributed to several interrelated factors. One of the primary drivers has been the increasing demand for resilient and cost-effective structures, spurred by heightened awareness of natural hazards, climate change, and urbanization. As societies recognize the need for more durable and adaptable infrastructure, PBD has emerged as a promising approach to meeting these requirements.

The growing body of experimental and analytical research on the performance of various structural systems, materials, and components has been instrumental in informing the development and validation of PBD methodologies. As our comprehension of structural behavior under different loading conditions continues to improve, our ability to refine and optimize PBD approaches also improves. In addition, advances in computational tools, numerical methods (e.g., the finite element method), and efficient phenomenological models [26,27] have played a crucial role in propelling PBD forward. These technological innovations have enabled more accurate and detailed modeling and analysis of structural behavior and performance under diverse loading conditions, equipping engineers with the tools necessary to effectively implement PBD methodologies. Recently, PBD was expanded to encompass additional natural hazards such as windstorms [28] and floods [29], as well as man-made hazards such as fire [30] and blast loads [31]. This expansion has led to the development of multi-hazard performance-based design methodologies [32], considering the intricate interplay between various hazards and structural systems and offering a comprehensive and integrated approach to structural design. As pointed out in [11], the two types of research, namely, experimental and analytical, required to support full implementation of performance-based seismic design are presented as follows for masonry walls and buildings.

3. Experimental Studies of Masonry Walls/Buildings

Masonry shear walls constitute a fundamental element of masonry buildings, serving to withstand lateral loads while ensuring structural stability and integrity. The primary function of a masonry shear wall involves the transmission of lateral forces from a building's roof and/or floors to its foundation. Contemporary masonry shear walls and buildings are typically designed by incorporating grout and various forms of reinforcement. The presence of such reinforcement enhances the structure's strength and ductility, enabling it to undergo large deformations and dissipate energy more effectively during seismic events, thereby mitigating the risk of structural damage or collapse. In the meantime, a large number of URM shear walls and buildings can still be found throughout the world, representing a significant aspect of cultural heritage. Due to their high mass, low stiffness, low ductility, and low strength, URM structures are more vulnerable to damage from earthquake-induced lateral loading. In this section, relevant experimental works performed since the 1980s to the present, focusing on the masonry shear walls (including the URM and RM shear walls) and/or buildings, are reviewed, and future experimental research needs to advance the PBD for masonry buildings are discussed.

3.1. Masonry Shear Wall Tests

3.1.1. Unreinforced Masonry Shear Walls

Throughout the 19th and early 20th centuries, unreinforced masonry (URM) walls designed using traditional methods constituted the most prevalent structural typology around the world [33]. Historically, masonry structures were built using trial-and-error processes without mathematical or predictive tools, relying on experience and craftsman-

ship. In recent decades, extensive experimental research on the URM shear walls has been conducted to gain valuable insights into their structural performance, including peak strength, ductility, energy dissipation capacity, failure modes, etc. This can potentially benefit improving code-based design and/or developing performance-based design.

Due to the heterogeneity and induced composite nature of masonry material, predicting the failure and collapse mechanisms of URM shear walls presents a significant challenge. The three primary failure modes for URM shear walls under in plane loading are diagonal tension cracking, shear sliding, and flexural rocking, as illustrated in Figure 2 with their corresponding force-deformation hysteresis loops. Diagonal tension cracking occurs when the principal tensile stress developed exceeds the tensile strength of masonry. In such cases, URM shear walls are characterized by rapid strength softening, stiffness degradation, moderate energy dissipation, and limited deformation capability, as shown in Figure 2a,b. Shear sliding is commonly initiated in cases with low frictional resistance and little cohesion. URM shear walls experiencing sliding failure exhibit a relatively stable, elastic-perfectly-plastic response, accompanied by high energy dissipation and displacement capacity, but usually characterized with relatively low strength, as demonstrated in Figure 2c,d. Flexural rocking failure is mostly observed in slender cantilever walls (i.e., height-to-length ratio is high) under a low axial load. Regarding the flexural controlled URM shear wall, damage is generally concentrated at top and/or bottom courses. Consequently, the in-plane response of flexural governed URM shear walls is close to nonlinear elastic, characterized by rocking behavior with limited hysteretic energy dissipation and considerable ductility, as evidenced in Figure 2e,f.

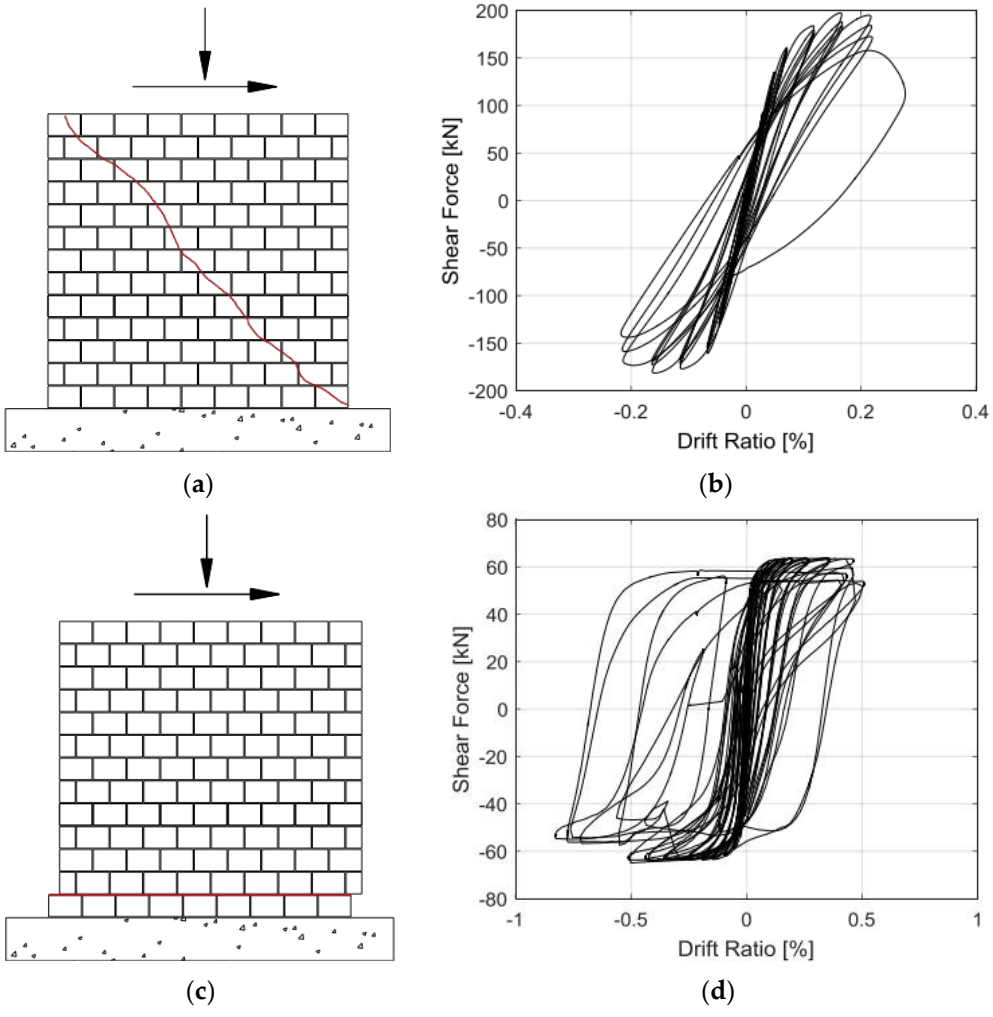

Figure 2. *Cont.*

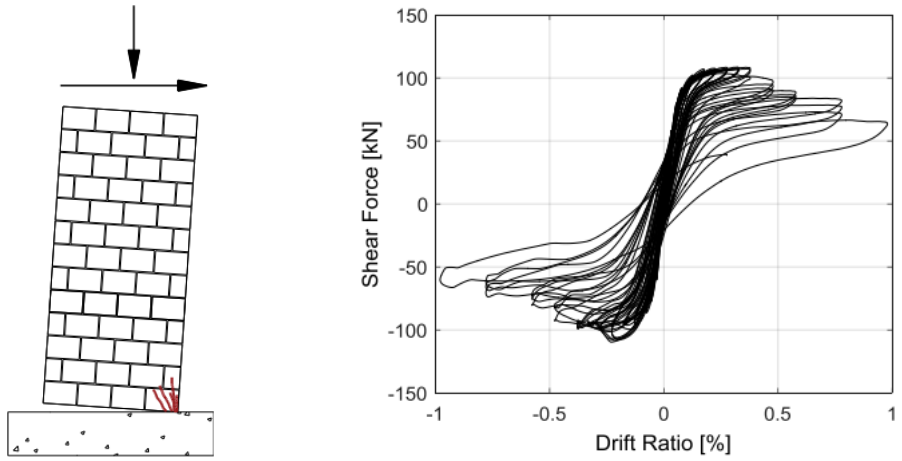

(**e**) (**f**)

Figure 2. Failure modes of URM shear walls and corresponding hysteresis loops: (**a**,**b**) diagonal tension failure, (**c**,**d**) shear sliding, and (**e**,**f**) flexural rocking failure (from [34]).

Two main types of masonry typologies were involved in the available experimental studies: conventional masonry made of solid brick units [35–44] and contemporary masonry made of hollow units [34,45–48]. These experiments revealed all the failure modes discussed previously, with several observed crack patterns shown in Figure 3. Notably, it is possible for two or more failure modes to interact concurrently, leading to a mixed failure mode, as demonstrated in Figure 3h,i.

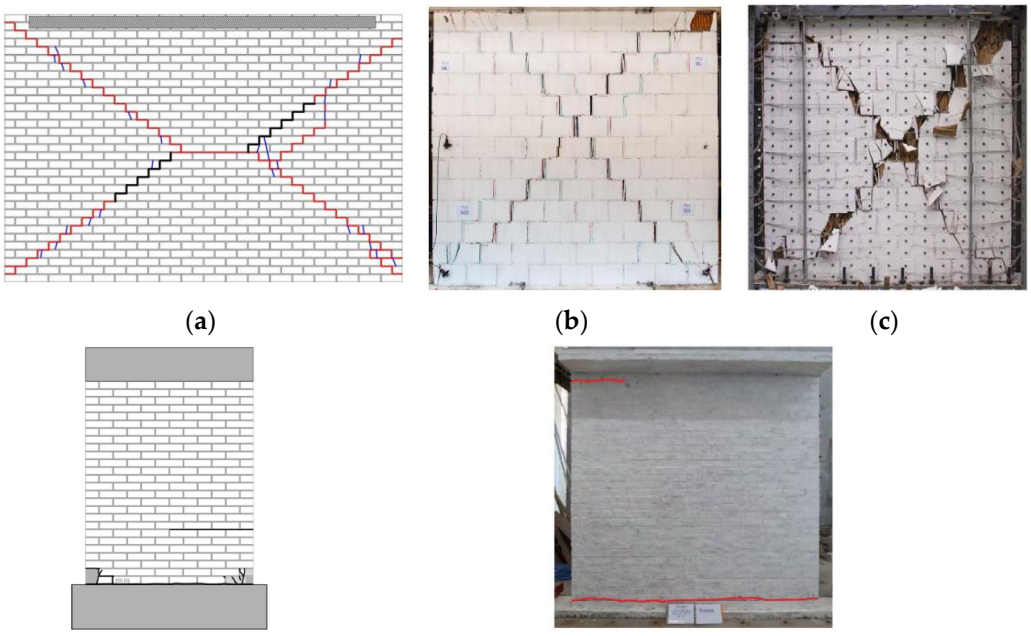

(**a**) (**b**) (**c**)

(**d**) (**e**)

Figure 3. *Cont.*

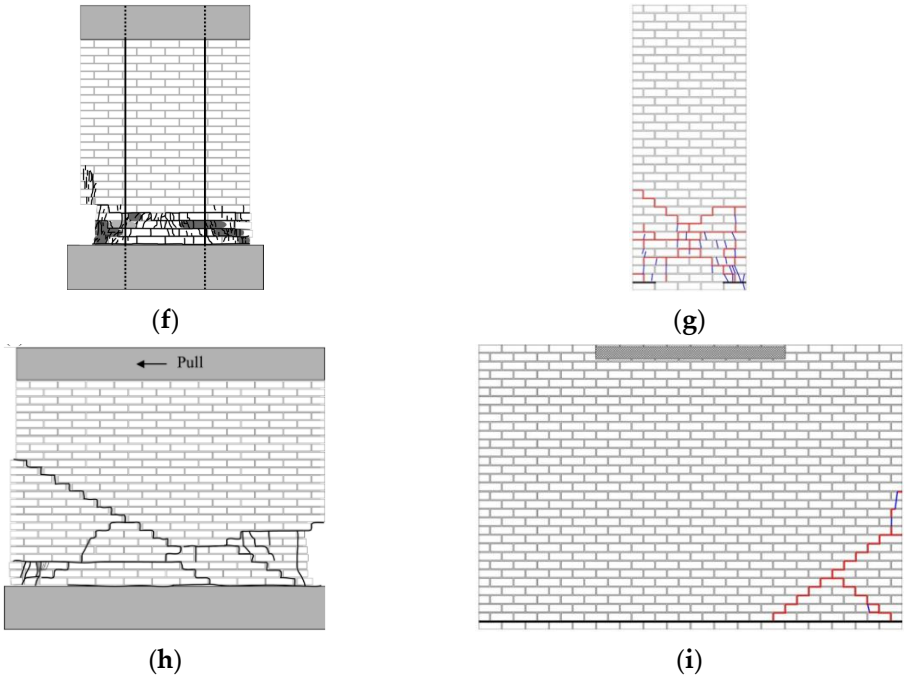

Figure 3. Failure modes observed in the experimental tests: (**a**–**c**) diagonal tension cracking [34,41,47], (**d**,**e**) shear sliding [39,43], (**f**,**g**) flexural rocking failure [39,41], and (**h**,**i**) mixed failure modes [39,41].

The majority of URM shear wall specimens were tested under static loading scenarios, including both monotonic and cyclic conditions, as summarized in Table 1. Towards a better understanding of failure mechanisms and structural performances of URM shear walls, researchers have typically examined the effects of potential influential variables: aspect ratio (i.e., height-to-length ratio), axial load, and boundary condition. With low aspect ratios, URM walls exhibit higher shear capacities and are more prone to shear-related failure modes (e.g., diagonal tension cracking and shear sliding [34,41,47]), while high aspect ratio walls are more susceptible to flexural rocking failure [39,41]. Increasing axial load would lead to an increase in the shear capacity of URM shear walls. This is due to the enhancement of frictional resistance under higher compressive stresses. However, as the axial load increases, URM shear walls become less capable of accommodating large deformations and exhibit reduced ductility [36,41].

Table 1. Summary about the experimental studies on the URM shear walls.

Masonry Typology *	Investigating Factor	Loading Protocol	Boundary Conditions	Reference
SU, SW	AR, AL	SC	C	[35]
SU, SW/PW	AL	SM	FF	[36]
SU, SW	AR	SC	FF	[37]
SU, SW	AR, AL	SC	FF	[38]
SU, SW	AR	SC	C	[39]
SU, PW	AR, AL	SC	C	[40]
SU, SW	AR, AL	SC	FF, C	[41]
SU, PW	AR, AL	SC	C	[42]
SU, PW	None	SC	C	[43]

Table 1. *Cont.*

Masonry Typology *	Investigating Factor	Loading Protocol	Boundary Conditions	Reference
SU, SW	AL	SM, SC	C	[45]
HU, SW	AL	SC	FF, C	[46]
HU, SW	AL	SC	Intermediate *	[47]
HU, SW	AR, AL	SC	FF, C	[34,48]
NA *	AR, AL	SC	FF	[49]
SU, SW	None	D	C	[44]

Masonry typology: SU (Solid Unit); HU (Hollow Unit); SW (Solid Wall); PW (Perforated Wall). Investigation factor: AR (Aspect Ratio); AL (Axial Load); Loading protocol: SC (Static Cyclic); SM (Static Monotonic); D (Dynamic). Boundary condition: FF (Fixed Fixed); C (Cantilever). Intermediate *: partial rotation constraint is enforced at the top of masonry wall specimen; NA *: relevant information is not available.

3.1.2. Reinforced Masonry Shear Walls

In comparison to conventional URM shear walls, RM shear walls demonstrate significantly enhanced structural performance. A RM shear wall is typically constructed of hollow concrete masonry units, and the grout is poured into the cavities. Steel reinforcing bars are placed within the units in vertical cells and horizontal courses. RM shear walls can be broadly classified into two categories: fully grouted reinforced masonry (FGRM) and partially grouted reinforced masonry (PGRM) shear walls. FGRM shear walls, characterized by all vertical cores of the masonry units being filled with grout, exhibit superior resistance to lateral loads and provide excellent bonding performance among masonry units, mortar, grout, and reinforcements. Conversely, PGRM shear walls involve grouting only selected vertical cores containing reinforcement bars, leaving the remaining cores hollow.

Similar to URM shear walls, RM shear walls typically exhibit three failure modes: flexural, diagonal, and sliding. Excessive cracking is not expected in RM shear walls due to the incorporation of reinforcements. For instance, vertical reinforcements could effectively delay the crack and damage propagation in the flexural governed walls. The in-plane capacity of shear governed RM walls can be significantly improved by inserting horizontal reinforcements. To enhance the understanding of the structural behavior of RM walls, a large number of experimental research projects were performed in the past few decades, as summarized in Table 2.

A test program on the seismic behavior of masonry single piers was initiated at the Earthquake Engineering Research Center of the University of California, Berkeley [20–23]. A series of experimental tests for RM walls were performed by varying the height-to-width ratio, grouting type (partially or fully), horizontal and vertical reinforcement ratio, and axial load. The specimens were designed to be double-fixed, which replicates the boundary conditions that masonry piers would experience in a perforated shear wall of a complete building. The axial load was found to significantly affect the hysteretic behavior of FGRM walls. Low axial loads favored the flexural failure mode, whereas the shear failure mode was commonly observed with high axial loads. On the other hand, horizontal reinforcements were found to be highly effective in inhibiting the opening of shear cracks and improving the ductility of masonry walls.

In the 1980s, a comprehensive research program was launched by the US–Japan Technical Coordinated Committee for Masonry Research (TCCMAR) [50] and aimed to address a wide range of topics, including loading protocols, masonry material tests, FGRM wall component tests, and full-scale building tests. More specifically, the influence of axial stress, shear span ratio, vertical/horizontal reinforcement ratios, tensile strength of reinforcing bars, and compressive strength of masonry on the structural performance of FGRM shear walls were experimentally investigated. With over 60 technical reports and papers documenting the findings (e.g., [51–60]), the TCCMAR program has laid the basis

for contemporary North American and Japanese masonry design codes (e.g., [8,9,61,62]). The experimental results [51,60] indicated that RM walls that exhibited a predominantly flexural failure (e.g., Figure 4a) were more ductile than those failing by diagonal shear cracking (e.g., Figure 4b). Moreover, increasing the horizontal reinforcement ratio could change the inelastic behavior from a brittle shear mode to a ductile flexural mode [55,56]. Conversely, the increase in axial load can severely undermine the flexural ductility due to the toe spalling, with the failure modes shifting from a mixed failure mode (e.g., Figure 4c) to a brittle shear mode [52,53,56].

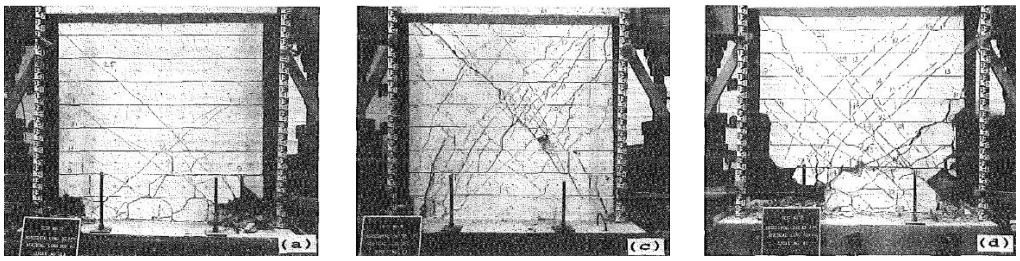

(**a**) (**b**) (**c**)

Figure 4. Experimental failure modes of FGRM shear walls as part of the TCCMAR program: (**a**) flexural failure, (**b**) shear failure, and (**c**) flexural–shear failure (from [52]).

The experimental study by Kikuchi et al. [63] examined the effects of aspect ratio, axial load, reinforcement ratio, and strengthening method on preventing the wall from sliding failure. A total of 19 FGRM shear walls were tested under a quasi-cyclic loading condition. Similar conclusions were obtained with respect to the benefits of axial load and reinforcement in improving the peak strength of FGRM shear walls. Moreover, the sliding strengthening by using dowel-reinforcing bars was found to be effective in preventing the masonry walls from sliding failure.

In order to assess the ductility of FGRM shear walls, six full-scale FGRM shear walls were tested under reversed cyclic lateral loading by Shedid et al. [64,65]. The test results showed that both wall drift at the onset of reinforcement yielding and wall ductility were highly dependent on the amount of reinforcement but only minimally affected by the level of axial load. Later, the experimental program was extended to investigate the influence of aspect ratio and boundary elements by testing seven additional half-scale FGRM shear walls [66]. A significant increase in ductility for the confined FGRM shear walls was observed.

Voon and Ingham [67] tested ten RM shear walls under static cyclic loading conditions, in which eight walls were fully grouted and the other two were partially grouted. The effects of reinforcement ratio, axial load, type of grouting, and wall aspect ratio on the wall's performance were studied. It was observed that the peak strength of RM shear walls decreased inversely in relation to the aspect ratio. The reinforcement not only provided additional shear resistance, but also improved the post cracking performance of the masonry walls when shear reinforcement was uniformly distributed up the height of the walls. Axial load could significantly improve the shear capacity of RM walls but be detrimental to the post cracking deformation capacities. The hysteretic behaviors demonstrated in Figure 5 showed that the flexural dominated wall was more ductile than the shear governed one. Compared with the FGRM walls, the PGRM walls exhibited significantly reduced capacities.

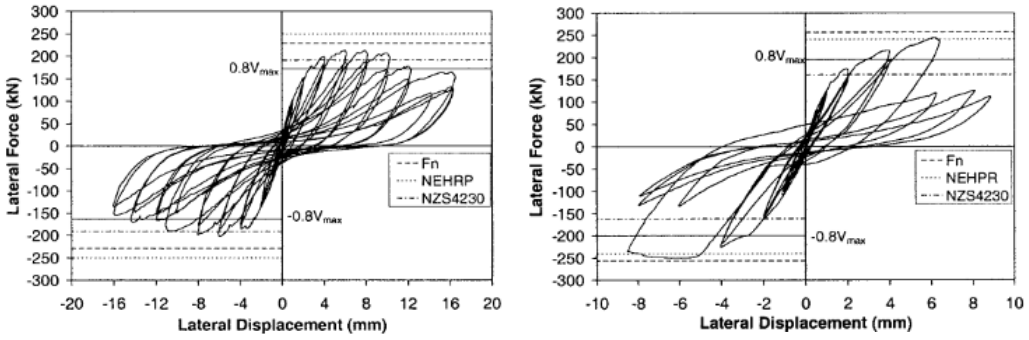

Figure 5. Hysteretic behaviors of FGRM shear walls governed by (**a**) flexural and (**b**) shear (from [67]).

During the years between 2010 and 2012, a joint research program "Performance-based seismic design methods and tools for reinforced masonry shear-wall structures" was launched by the University of California San Diego, the University of Texas at Austin, and Washington State University, in which a total of 41 FGRM shear walls were tested under quasi-static cyclic loading conditions [68–72]. Factors such as aspect ratio, boundary condition, axial load, and reinforcement ratio were investigated. Test results [68–72] showed that cantilever walls tended to be governed by flexural behavior, associated with significant flexural cracking, yielding of vertical reinforcement, degradation of compressed toe, inelastic bulking of vertical reinforcement near the base, spalling of the toe regions, etc. Similar to the test results reported from the TCCMAR program, walls with lower aspect ratios and lower axial loads exhibited larger deformations from sliding and shear. Walls exhibiting flexural behavior had larger plastic hinge zones and dissipated more energy than walls with other failure modes, including a mixed flexural/shear/crushing failure mode. In general, as the vertical reinforcement ratio increased, displacement ductility decreased. However, different from those findings reported in the TCCMAR program, the magnitude of the applied axial load did not appear to have significant impacts on the deformation capacity, as noted in [68].

Zhao and Wang [73] tested ten FGRM shear walls, of which four were designed for shear failure and six for flexural failure. The experimental results indicated that the increases of amount of horizontal reinforcement and axial load significantly improved the peak strength. Flexural governed walls experienced less stiffness degradation than walls governed by shear. More recent experimental studies can be found, e.g., Siyam et al. [74], and Seif ElDin and Galal [75,76], which illustrated the effects of axial load, shear span to depth ratio, and amount of horizontal and/or vertical reinforcement on the structural performance of FGRM shear walls. Other than (quasi) static loading conditions employed in the previously discussed experimental studies, Mojiri et al. [77] performed the shake table tests on lightly reinforced FGRM shear walls with the aim of developing codes in North America for reinforced masonry structures. The test results demonstrated the capability of lightly reinforced RM shear walls to adequately dissipate energy through nonlinear flexural response. Then, an analytical model was calibrated using the obtained experimental data [78], and fragility curves were developed as an essential component of PBD.

The previously reviewed works focused on the FGRM shear walls. As a cost-effective alternative in modern lateral force-resisting systems, PGRM shear walls have gained increasing attention in recent years, due to their many advantages, such as reduced weight, improved thermal insulation, enhanced fire resistance, and greater design flexibility.

The experimentally investigated variables for understanding the structural performance of PGRM shear walls are similar to those for FGRM shear walls, such as aspect ratios [79–85], amount and/or detail of reinforcement [79–82,84–94], axial load levels [79,83,84,95–97], and boundary conditions [97]. In particular, grouting detailing (e.g., grouting space/ratio, grouting type) is the key aspect frequently investigated in PGRM

shear walls [83,91–93,96–98]. These experimental results were used, on the one hand, to examine the performance of current prescriptive code provisions. For instance, Calderón et al. [85] evaluated the performance of the Canadian Masonry Design code [8], the American Masonry Design code TMS [9], and some other empirical analytical models [51,99] by using experimental data. The comparison indicated that none of these models estimated the peak strength of PGRM shear walls appropriately. Elmapruk [91], Minaie et al. [97], and Nolph and ELGawady [93] concluded that the Masonry Standards Joint Committee (MSJC) [61] overestimated the shear strength of PGRM shear walls by comparing the experimental results with the design code expressions. On the other hand, these experimental data can potentially be used in the next generation of the PBD framework to develop the fragility functions. Numerous test results (e.g., [81,83,87]) showed that the PGRM shear walls were capable of providing adequate ductility and sufficient energy dissipation, thus having a significant potential of becoming a predominant structural typology in low to moderate seismic zones.

Table 2. Summary about the experimental studies on the RM shear walls.

Grout Type	Loading Conditions	Boundary Conditions	Reference
F, P	SC	FF	[20–23]
F	SC	C	[51–60,64–66,73,75,76]
F	SC	FF	[63]
F, P	SC	C	[67]
F, P	SC	FF, C	[68–72]
F	SC	NA *	[74]
F	D	C	[77]
P	SC	C	[79]
P	SM, SC, D	C	[95]
P	SC	FF	[80]
F, P	SC	C	[81,82]
P	SC	NA *	[91]
P	SC	C, FF	[97]
P	SC	C	[83–86,88–90,92–94]
P	SM	C	[98]
P	D	C	[87]

Grout type: F (Fully Grouted); P (Partially Grouted). Loading protocol: SC (Static Cyclic); SM (Static Monotonic); D (Dynamic). Boundary condition: FF (Fixed-Fixed); C (Cantilever). NA *: relevant information is not available.

3.2. Building System Tests

While the experimental studies at the component level provided valuable insights, masonry building system performance has not been sufficiently explored. The complexity of component-level response is further magnified at the system level, taking into account additional aspects that possibly impact the overall behavior of masonry building systems, such as building configuration, presence of openings, structural irregularities, stiffness compatibility of adjacent components, in-plane and out-of-plane stiffness of floor diaphragms, etc.

The vast majority of experiments at the masonry wall component level were conducted under (quasi) static conditions. Such tests present several benefits, including their relative simplicity in execution and control, cost-effectiveness, and the ability to clearly identify failure modes and mechanisms. However, (quasi) static tests are incapable of representing the effects of dynamic loading, such as the scenario of seismic events, which may possibly lead to conservative results, as noted in [100,101].

Compared to component-level tests, system-level tests are much more costly and time-consuming, and only limited experimental studies on the system level were available. Yi et al. [102] tested a two-story URM building with timber floor and roof diaphragms under static loading conditions, aiming to validate extrapolating from individual component behavior to the overall response of a URM building system. The tested URM building exhibited a large initial stiffness, but a significant stiffness decrease was followed by even a small increasing lateral drift. Paquette and Bruneau [103] and Cohen et al. [104,105] investigated the influence of flexible roof diaphragms on the URM and RM buildings, respectively. The test results by Paquette and Bruneau [103] showed that the weak diaphragm still remained elastic without significant strength degradation, even with large deformations. The RM building test [104,105] found that seismic damage in walled structures with flexible diaphragms cannot be completely characterized by the inter-story drift ratios of the walls, which are also dependent on the diaphragm drift ratio and correlated to diaphragm and wall damage.

Aldemir et al. [101] investigated the structural performance of existing two-story masonry buildings by applying cyclic lateral loading up to near collapse utilizing two hydraulic jacks at each story level. A significant stiffness loss after a drift ratio of 0.1–0.2% and considerable strength degradation at a drift ratio of 0.5% were observed, reflecting a relative brittle performance. The dominant failure mode for each wall was diagonal tension failure, shown in Figure 6.

Figure 6. Damage distributions of the tested two-story masonry building (from [101]).

Mendes et al. [106] tested two masonry buildings under seismic loading with increasing amplitude. One specimen is an existing building, and the other is strengthened by steel to improve the connection between walls and flexible floors, as illustrated in Figure 7a,b. Figure 7c,d shows the test results: the non-strengthened masonry building presented substantial damage with a higher concentration of damage at façades in almost all spandrels, while the strengthened masonry building demonstrated moderate damage, verifying that the strengthening elements improved the seismic performance of the buildings. Avila et al. [107] tested two masonry buildings (one reinforced and one unreinforced) under incremental seismic input motions in two orthogonal directions. The structural behavior of these two buildings was rather different. For the RM building, the damage was only concentrated on the first floor. Regarding the URM building, long horizontal cracks developed

and propagated, dividing the whole building into several macro blocks, eventually leading to relative sliding. A similar study aiming to investigate the behavioral difference between the URM and RM buildings was conducted by Tomazevic [108], with the crack pattern shown in Figure 8. Both studies reached the conclusion that the RM buildings considerably outperformed the URM buildings in terms of the strength, ductility, and energy dissipation capability.

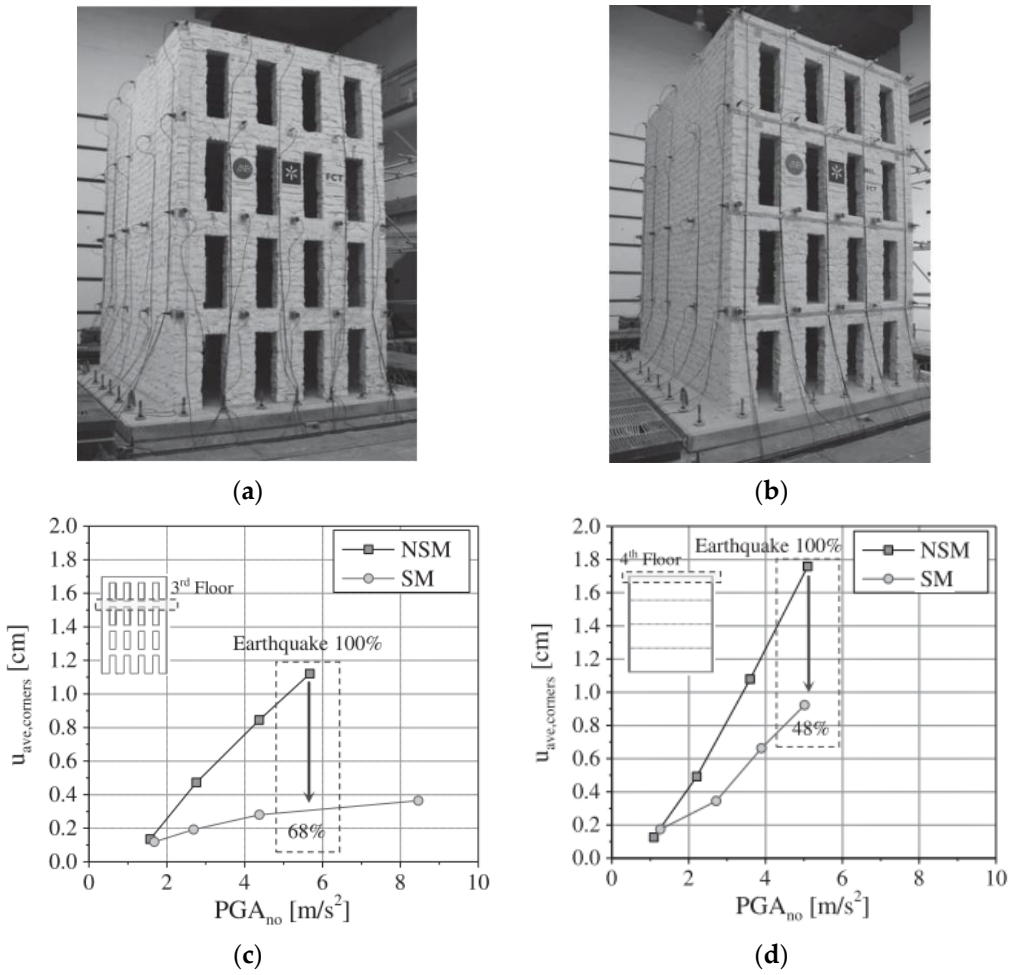

Figure 7. (**a**,**b**) Non-strengthened and strengthened URM building specimens, and (**c**,**d**) comparison of the average out-of-plane relative displacement with respect to the corners at the 3rd floor of the facades and 4th floor of the gable walls (from [106]). NSM: Non-strengthened masonry; SM: Strengthened masonry.

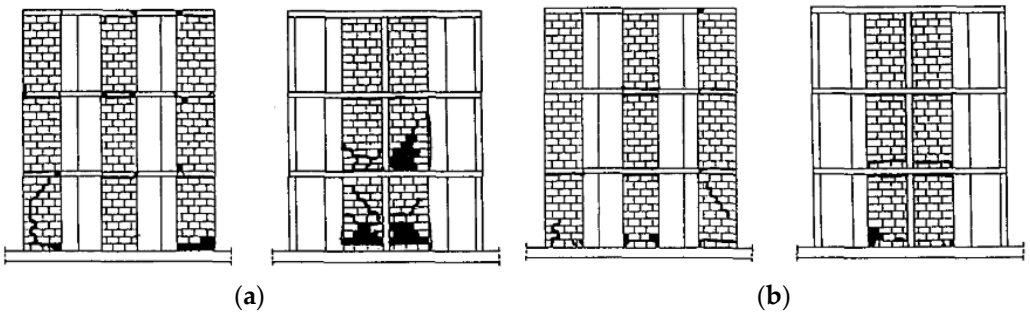

Figure 8. Damage distributions for the (**a**) URM building and (**b**) RM building (from [108]).

As a part of the collaborative project "Performance-based seismic design methods and tools for reinforced masonry shear-wall structures", Mavros et al. [109,110] tested a two-

story FGRM building on the shake table, as shown in Figure 9a. Even at the ultimate stage, the building did not collapse, although it experienced severe damage and incurred diagonal cracking. An important conclusion based on test data is that within the whole building, the walls in the orthogonal direction had a significant contribution to the lateral load resistance of the structure as they exerted axial compression through the horizontal diaphragms and lintels on the wall components parallel to the loading direction, implying the conventional force-based design method could result in unsatisfactory performance. Later, Stavridis et al. [111] performed another shake table test on a three-story FGRM building, with the test specimen shown in Figure 9b. The building was subjected to a series of dynamic loadings, including nine seismic excitations, with some intensities exceeding the maximum considered earthquake used in the design. The structure exhibited a considerably higher base shear capacity than the design one, with little or no damage except for the last two high intensity excitations.

(**a**) (**b**)

Figure 9. Shake table tests at University of California, San Diego: (**a**) two-story RM building (from [110]) and (**b**) three-story RM building (from [111]).

To further investigate the performance of PGRM buildings, Koutras and Shing [112] tested a full-scale, one-story PGRM building at the University of California, San Diego. The specimen was designed for a moderate seismic zone according to code provisions. The experimental results showed that the tested building was able to develop an adequate base shear capacity and withstand earthquake motions that had an effective intensity of two times the maximum considered earthquake loading. Only moderate cracking in mortar joints was observed. However, different from the FGRM building tests [109–111], the PGRM specimen eventually failed in a brittle manner [112], showing that the PGRM building is inferior to that of the FGRM building in terms of deformation capability.

More recently, a research project "Collapse Simulation of Shear-Dominated Reinforced Masonry Wall Systems" was conducted at the University of California, San Diego. The main focus of this project at the building level is twofold: (1) to investigate the influence of coupling forces introduced by horizontal diaphragms on the strength and deformation capability of the structural system, and (2) to study the influence of non-seismic load-carrying walls and columns on the drift capacity and collapse resistance. Two full-scale single story FGRM specimens were tested [113]. The difference between the two designed specimens is that the second specimen had six additional planar walls perpendicular to the direction of shaking, as shown in Figure 10. The benefits of additional planar walls were verified by a higher lateral resistance and a much lower drift ratio at comparable ground motion levels, as exhibited by Specimen 2. It was concluded that [113] the observed higher displacement capacities can be largely attributed to the presence of wall flanges by comparing the previous experimental results on shear-dominated planar wall segments (e.g., [51,67,68]).

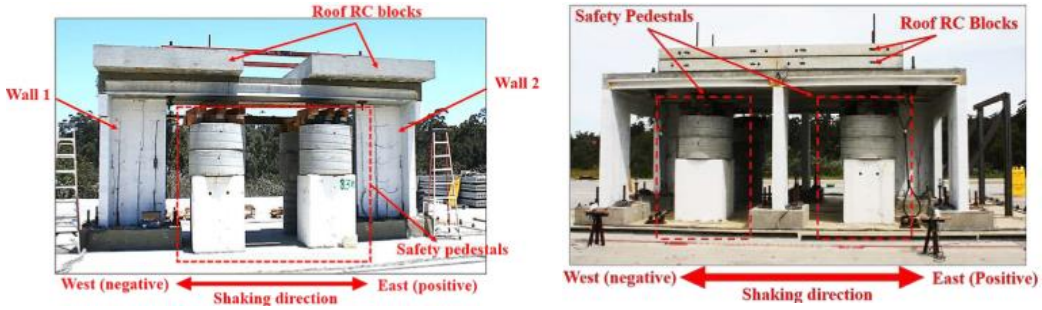

(**a**) (**b**)

Figure 10. Shake table tests at University of California, San Diego: (**a**) Specimen 1 (without flanges wall) and (**b**) Specimen 2 (with additional flange walls) (from [113]).

3.3. Future Research Needs

Upon reviewing the experimental works and their associated conclusions discussed above, it is evident that a rich experimental database of masonry walls (including URM, FGRM, PGRM) is available. Although most tests were conducted under cyclic loading conditions, many studies have only reported strength-related structural characteristics. Quantitative assessments of additional factors, such as ductility, energy dissipation capability, and stiffness degradation, were less reported during data post-processing procedures. Addressing these factors is particularly important for a reliable evaluation of the structural performance of masonry walls, considering that strength-based approaches are not adequate to recognize the actual performance of masonry walls. Furthermore, the development of experimentally based fragility functions, which is a key component of the implementation of the PBD framework, relies heavily on the compilation of such experimental information.

At the building level, experimental data remain limited due to the restrictions of test equipment and space. Consequently, a significant knowledge gap still exists in comprehending the structural response of masonry buildings. The intricate interaction effects (e.g., building twist, load redistribution) between different structural components (e.g., shear wall, floor, column) and/or nonstructural components (e.g., parapet wall, partition wall, door/window) are further intensified by complex external loading scenarios. This complexity is also the primary reason why wall segments with identical material constituents and geometries tested individually and within a building may exhibit different behaviors. Moreover, there is currently no general agreement on how to interpret the experimental data from the component level to the building level. For instance, quantifying the displacement ductility at the component level is rather simple, usually taking as the ratio between the measured top displacements at a specific state beyond yielding (such as 20% strength loss) and at yielding of the structural component. However, in a masonry building composed of walls with different configurations, this procedure is not simple. Heerema et al. [18] made several attempts in this regard based on different approaches: (1) averaging the ductility values of all walls aligned along the loading direction, and (2) weighted average approach corresponding to the wall strength contribution to the overall building strength at different drift levels. Nonetheless, both methods led to overestimated predictions. Future experimental research programs should be well designed to address this gap, enabling a feasible performance prediction at the building level through component level information.

However, it is unrealistic to expect the same amount of experimental information for masonry structures at the component and building levels or implement experimentally based fragility functions within the PBD framework. The available experimental data should be thoroughly collected and analyzed for the validation and calibration of practice-oriented numerical or analytical models, which will be discussed in the next section.

4. Numerical Studies of Masonry Walls/Buildings

PBD will realize its full potential only if robust data on the expected or predictive performance of most (if not all) structural components (e.g., masonry shear walls) and systems (e.g., masonry buildings) are available. This can be accomplished through experimental tests, as reviewed in the previous section. However, it is impractical to follow the PBD implementation procedure for all masonry buildings through experimental tests due to economic concerns. To complement experimental methodologies, numerical approaches have been proposed to investigate or predict the structural performance of masonry shear walls and building systems under various loading scenarios. In general, numerical modeling approaches can be classified into two groups depending on different levels of sophistication and simplification: micro modeling and macro modeling approaches [114].

The micro modeling approach for masonry structures can be further divided into detailed and simplified micro modeling approaches. In the detailed micro modeling approach, units and mortar are represented with solid continua, while the contact surfaces between the units and mortar are modeled by discontinuous cohesive interfaces. In the simplified micro modeling approach, mortar and unit–mortar contact surfaces are lumped into mortar joints modeled by zero-thickness interface elements. Consequently, the number of interface elements considered in the simplified micro model is decreased, resulting in reduced computational costs.

Conversely, the macro modeling approach treats masonry as an averaged continuum using homogeneous constitutive laws without explicit modeling of the geometry and material of individual constituents (i.e., masonry units, mortar, and joints). As such, macro modeling is computationally efficient and applicable for masonry structures with sufficiently large dimensions. In this section, relevant numerical studies on using micro and macro modeling strategies are reviewed, including the pioneering work (e.g., [115]) and the latest ones (e.g., [116]).

4.1. Micro Models

4.1.1. Unreinforced Masonry Shear Walls and Buildings

The (simplified or detailed) micro modeling approach was initially widely employed for the modeling of masonry components (e.g., unit–mortar–unit assemblage, masonry triplet) and URM shear walls. As the key aspect of micro modeling, interface models used for simulating mortar joints have received great attention within the masonry community. To achieve a high-fidelity interpretation about the composite nature of masonry structures and further reasonably capture the structural performance of masonry shear walls and systems, various failure modes that possibly occurred within the mortar joints should be well considered.

In general, there are two groups of interface modeling for simulating mortar joints. The first group considered two main failure modes, i.e., tensile cracking and shear sliding, by using one or two yield surfaces in constitutive model formulations (see for example [117–122]). The second type of modeling approach incorporated the compression-related failure in addition to the two aforementioned failure modes [116,123–133]. These interface models were formulated in rigorous computational mechanics (e.g., plasticity-based, damage-based, damage-plasticity-based) frameworks. A comprehensive review of interface model formulations is beyond the scope of this work, and interested readers are referred to [134]. In this study, the validations and/or applications of micro models developed relying on these interface models on the performance of masonry shear walls and buildings is the focus.

Typically, developed micro models are first validated using existing experimental results. Remarkable success was achieved in reproducing the structural behaviors of URM shear walls, including the load-deformation behaviors and failure modes. Most current studies based on the micro modeling approach focused solely on the monotonic behavior of URM shear walls (e.g., [116,117,120–129,131–133,135–146]). For instance, URM shear walls tested in the static monotonic loading condition [36], characterized by a typical diagonal tension failure mode, were widely used as validation examples in a large number of studies,

e.g., [121–123,132], shown in Figure 11. The validation results indicated the capability of these developed micro models to predict the initial stiffness, peak strength, and possible post-peak behavior.

Nonetheless, a relatively small number of studies focused on the cyclic behavior of URM shear walls [119,130,147–154], partly due to the significant numerical complexity of theoretical implementations. The development of a cyclic constitutive model of mortar joints should incorporate the main features of the hysteretic stress–strain loop of the material: energy dissipation during a cycle, plastic strains at the zero-stress level, crack closure under compressive stresses, and both strength and stiffness degradation in the tensile and compressive regimes. For instance, the flexural failure modes of URM walls tested in [37,41] and their corresponding hysteretic loops were reasonably predicted using the micro modeling strategy, as evidenced by studies [149,150], illustrated in Figure 12.

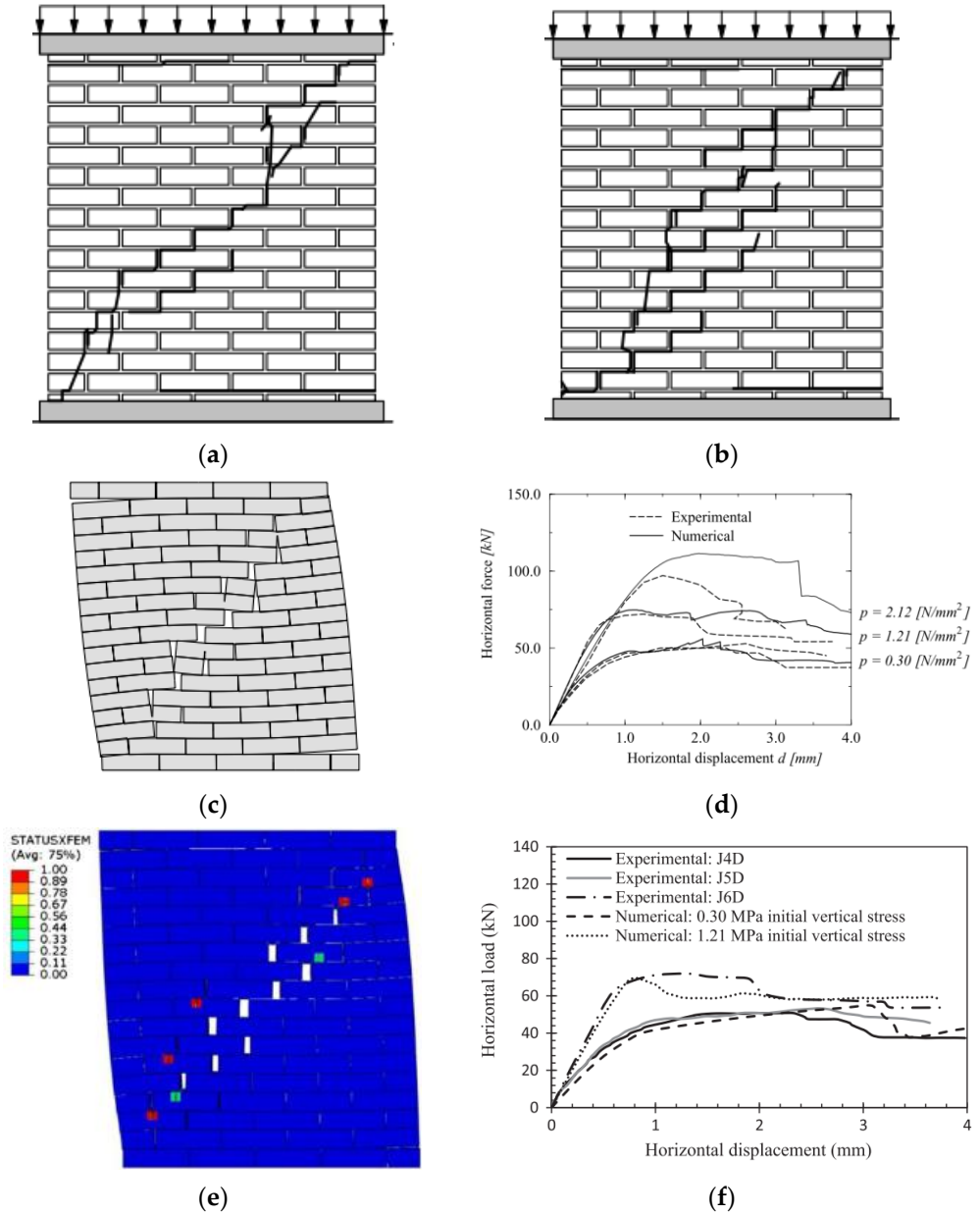

Figure 11. *Cont.*

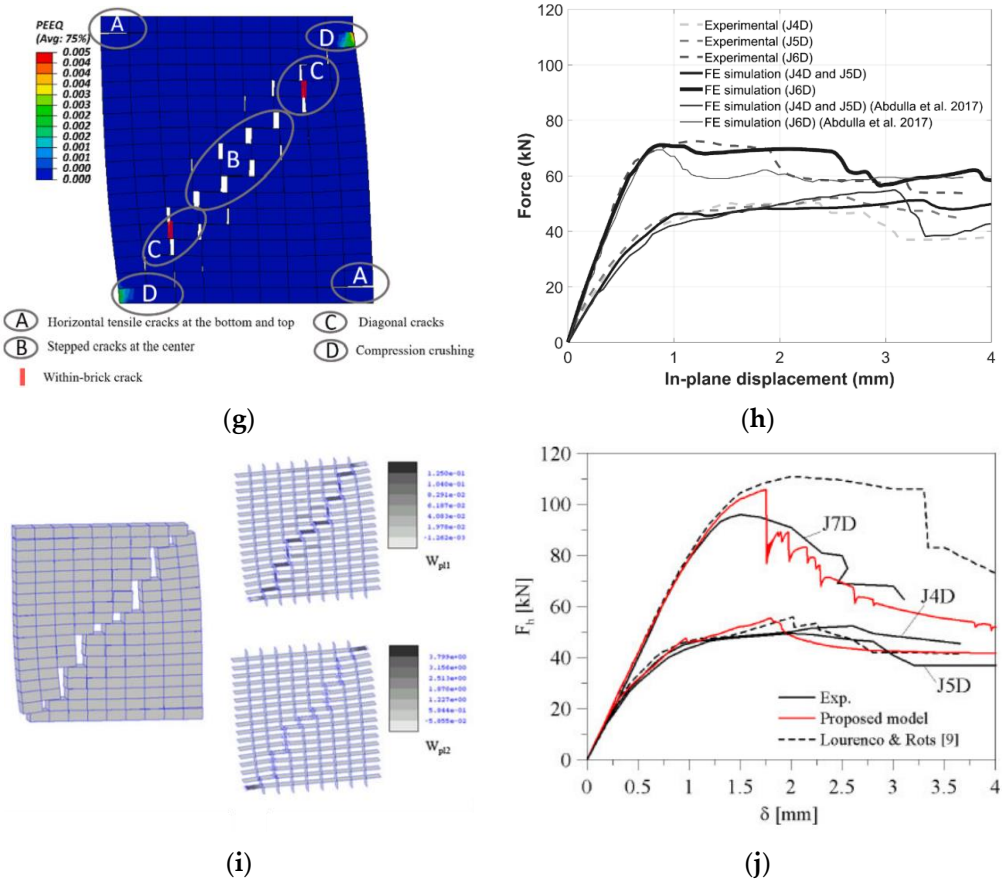

Figure 11. (**a**,**b**) Failure modes of tested URM shear walls [36], and (**c**–**j**) experimental–numerical comparison in terms of the failure modes and horizontal deformation-load behavior from Lourenco [124], Abdulla et al. [121], Zeng et al. [122], and Macorini and Izzuddin [132].

While the micro modeling strategy has achieved significant success in predicting the performance of URM shear walls under the (quasi) static conditions, its application to the dynamic loading scenarios (e.g., seismic loading) remains rather limited [149]. Furthermore, at the building level, the micro modeling strategy is evidently infeasible due to the intense computational cost and challenge in the determination of required material parameters, with only one study published recently [155].

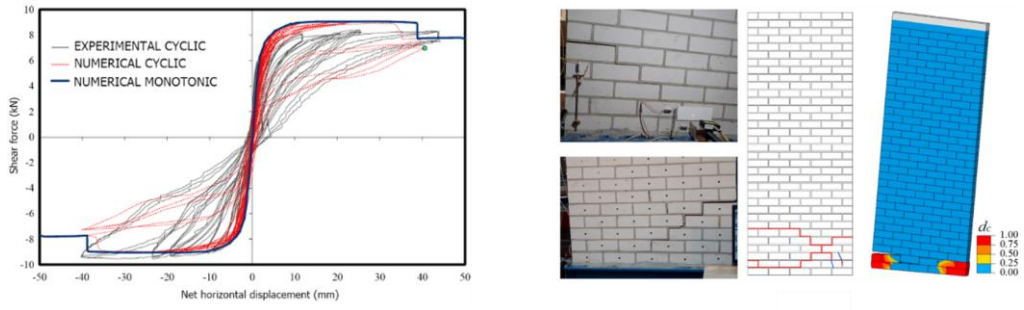

Figure 12. *Cont.*

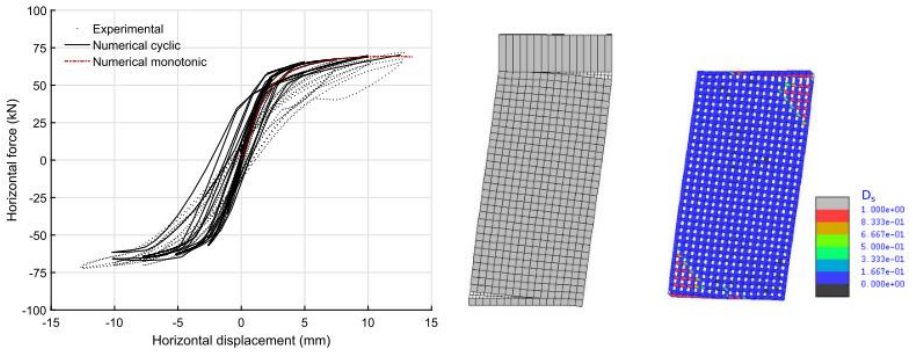

(**b**)

Figure 12. Flexural rocking failure and corresponding hysteretic behaviors of URM shear walls predicted by the micro modeling strategy: (**a**) D'Altri et al. [151] and (**b**) Minga et al. [149].

4.1.2. Reinforced Masonry Shear Walls and Buildings

Shing and Cao [156] made an early attempt to simulate PGRM shear walls using the micro modeling strategy. The masonry units were simulated using a plane-stress smeared crack formulation, and mortar joints were modeled by an elastic–plastic interface model developed by Lotfi and Shing [117]. No relative slip was assumed for the reinforcement-grout interface. The validation results illustrated that the lateral strengths obtained in the simulations were higher than those shown by tests. The discrepancies were attributed to the different load histories (i.e., monotonic or cyclic) and partly to the assumption in the bond strength between the wall panels and concrete head beams.

In recent years, more high-fidelity micro models have been developed by researchers for the modeling of modern RM shear walls. Maleki [81] simulated the PGRM shear walls in a discrete manner by using smear-crack plane stress elements to represent the grouted parts and cohesive interface elements to model the ungrouted parts and mortar joints, respectively. The proposed modeling scheme was capable of capturing the cracking pattern but was only applicable to monotonic loading scenarios.

Bolhassani et al. [157] used the concrete damage plasticity (CDP) model [158] to simulate the plastic behaviors of units and grout, and a cohesive contact-based surface was employed to represent the cracking behaviors of head and bed joints. For other possible interactions, perfect bonding (i.e., no relative slip deformation) was assumed for steel-grout and grout–unit interactions. The validation results showed that the developed model was capable of predicting the peak strength of PGRM shear walls.

Calderón et al. [159–161] developed micro models for PGRM shear walls, as shown in Figure 13. The nonlinear behaviors of units, mortar, and grout were considered by means of a total strain-based crack model, which accounted for the tensile cracking and compressive crushing. The steel reinforcement was assumed to be perfectly bonded with the surrounding grout parts and represented with beam elements and the Von Mises plasticity model. The proposed modeling strategy involved the nonlinear behaviors of the following interactions: unit to head-joint, bed-joint to head-joint, bed-joint to reinforcement, unit to grout, and bed-joint to grout. The main challenges presented here were related to the determination of material parameters for different interaction properties. Some material parameters were determined based on the experimental results, while most are assumed based on empirical relationships (e.g., from Model Code [162]). Numerical validations included several PGRM shear walls with or without openings, and reasonable agreements were achieved in terms of failure modes, lateral resistances, and deformation capacities. However, the developed models were not able to handle the cyclic loading conditions.

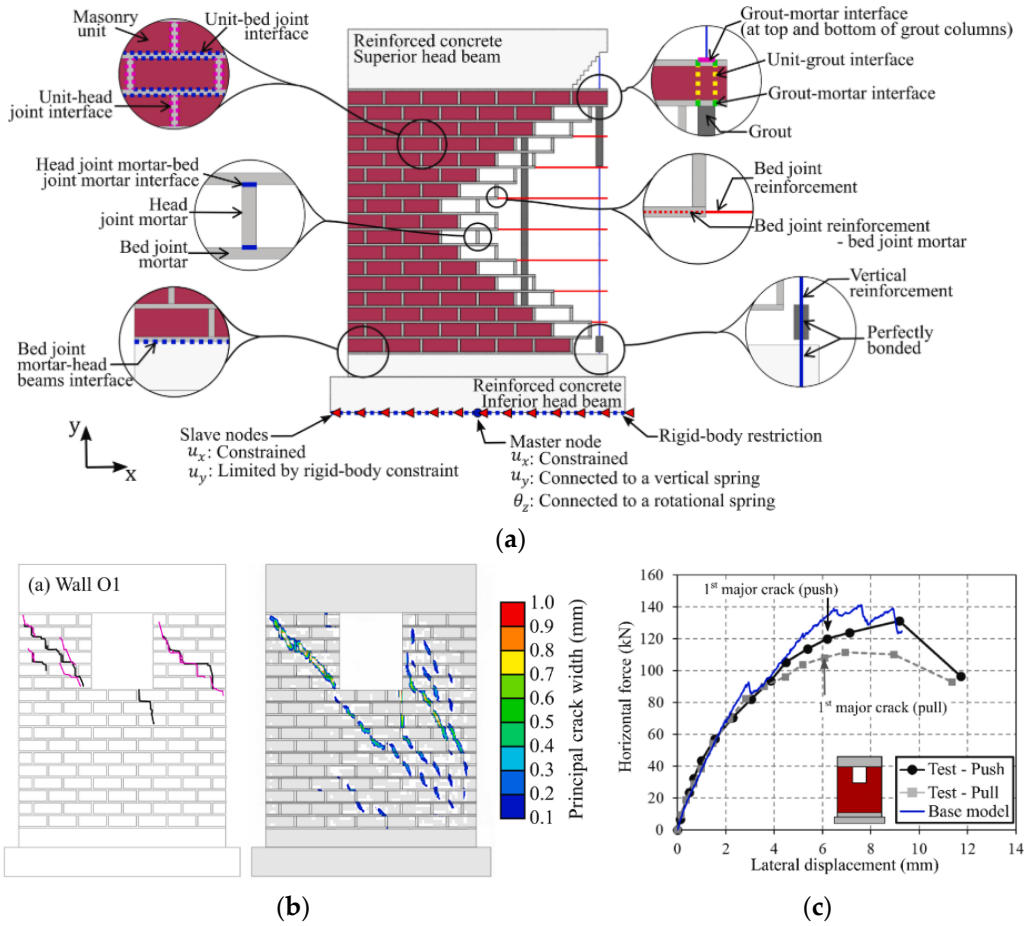

Figure 13. (**a**) Micro modeling strategy and (**b**,**c**) numerical–experimental comparison in terms of the crack pattern and load-deformation behavior for Wall O1 by Calderón et al. [160].

The developed micro models by Calderón et al. [159–161] were subsequently used for a parametric study to assess the influence of aspect ratio, axial load level, and horizontal reinforcement ratio on the behaviors of PGRM shear walls [163]. The analysis results indicated that increasing the horizontal reinforcement ratio could be associated with spreader damage and narrower cracks. Meanwhile, increasing the aspect ratio results in higher deformation capability and lower strength.

Mavros [109] proposed a new discretization scheme for the micro modeling of FGRM shear walls. Smear-crack shell elements were used to simulate the concrete compressive behavior, and cohesive discrete crack interface elements were placed at 45 and 135 degrees to capture the possible diagonal shear cracks in the units. Reinforcing steel was modeled with truss elements that were connected to the smear-crack shell elements through the nonlinear bond-slip and dowel action interface elements. The developed model was validated using existing experimental walls, including flexural- and shear-governed FGRM walls. The simulation results were in good agreement with the experimental results in terms of failure mechanisms, hysteretic behaviors, energy dissipation, stiffness, and strength of the walls. The proposed modeling scheme was later proven to be capable of predicting the complex three-dimensional behavior of a two-story masonry building tested on the shake-table in the same work [109]. The damage distribution and drift time history obtained by simulation match very well with the experimental ones.

Koutras and Shing [164,165] improved the modeling scheme proposed by Mavros [109] in the following ways: (1) adding horizontal and vertical cohesive interfaces to account for possible sliding and splitting failure of masonry, respectively; (2) accounting for reinforcement buckling by using beam elements instead of truss elements while also considering the flexural deformation. The modeling discretization proposed by Koutras [164,165] is shown

in Figure 14, leading to accurate predictions for the structural performance of FGRM wall components under static cyclic loading and RM buildings under dynamic loading. Moreover, Koutras and Shing [164,166] extended the applicability of the proposed modeling scheme from FGRM walls to PGRM walls. The grouted part of PGRM walls was modeled in the same way as that of FGRM walls, while the ungrouted units were represented by quadrilateral three-layered shell elements with vertical and horizontal interfaces inserted. It is worth noting that only the thickness of face shells of units was considered in the shell elements. The validation results indicated the significant potential of the proposed modeling scheme to accurately capture the performance details of PGRM shear walls and buildings, including the hysteretic behaviors, failure modes, drift ratio time history, etc.

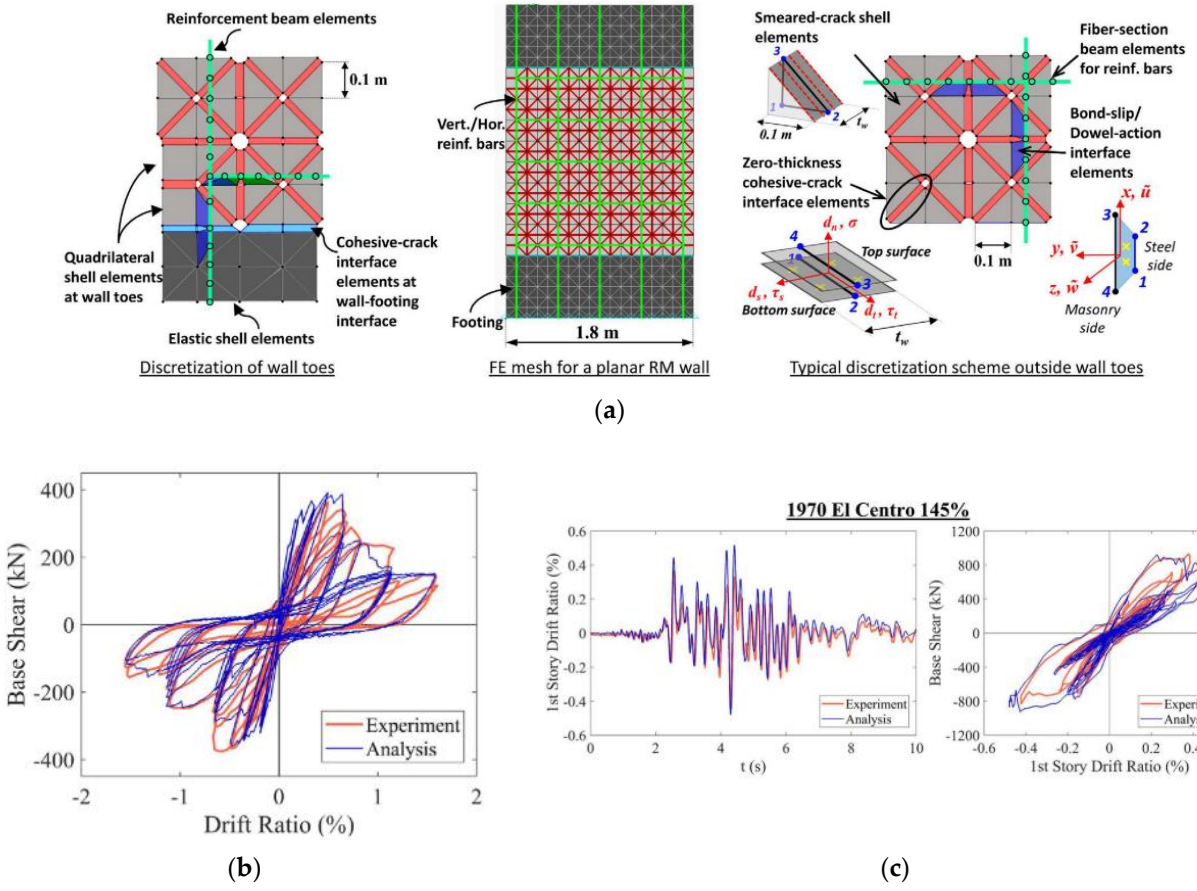

Figure 14. (**a**) Improved micro modeling scheme for FGRM shear walls, (**b**) experimental–numerical comparison in terms of the base shear-drift ratio for a FGRM shear wall, and (**c**) experimental–numerical comparison in terms of the drift ratio time history and base shear–drift ratio relationship for a RM building (from [165]).

Elmeligy et al. [167] developed finite element models based on the micro modeling strategy in VecTor2 software [168] to simulate the cyclic behaviors of PGRM shear walls. The developed models neglected the interfacial effects between the grouted units, while the shear and tensile failures at the block–mortar interfaces of ungrouted units were taken into account. Good agreements were reached between the experimental and numerical results with respect to some common engineering demand parameters (EDPs), e.g., ultimate load, displacement at ultimate load, displacement at 20% strength degradation, dissipated energy, and displacement ductility. Subsequently, a comprehensive parametric study was conducted to study the sensitivities of different masonry material properties on the EDPs. The sensitivity analysis revealed that ungrouted masonry properties, especially the angle of internal friction, are the most influential on the behavior of the walls for nearly all investigated EDPs. In addition, a comparison of the structural behaviors of FGRM and

PGRM shear walls was performed. The simulation results shown in Figure 15 indicated that more inclined cracks were developed in PGRM shear walls compared with FGRM shear walls. FGRM shear walls had a higher ultimate load and a lower corresponding displacement than their PGRM counterpart walls.

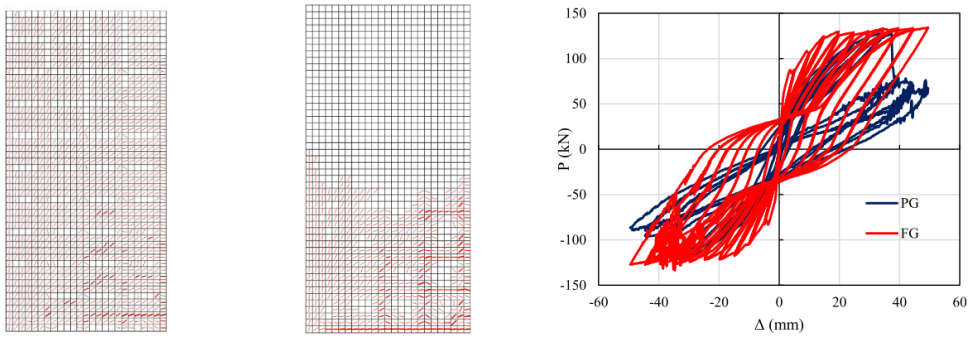

(**a**) (**b**) (**c**)

Figure 15. (**a**,**b**) Crack patterns of PGRM and FGRM shear walls, respectively, and (**c**) comparison of hysteretic behaviors for PGRM shear walls and their counterparts (from [167]).

4.2. Macro Models

Macro models for masonry structures can be roughly categorized into two types: macro continuum and macro element models. In macro continuum models, masonry is represented as a continuum deformable body with a fictitious homogenized isotropic or orthotropic constitutive law. The constitutive law is typically formulated in the various computational mechanics frameworks, such as damage-based [169–175], plasticity-based [176–180], and damage-plasticity-based [181–186]. Consequently, the mesh discretization in macro continuum models does not need to describe the actual masonry texture. The computational cost is moderate and generally lower than that of micro models, enabling a more efficient procedure for large-scale masonry structural analysis. Figure 16 shows some examples of macro modeling of masonry shear walls and buildings.

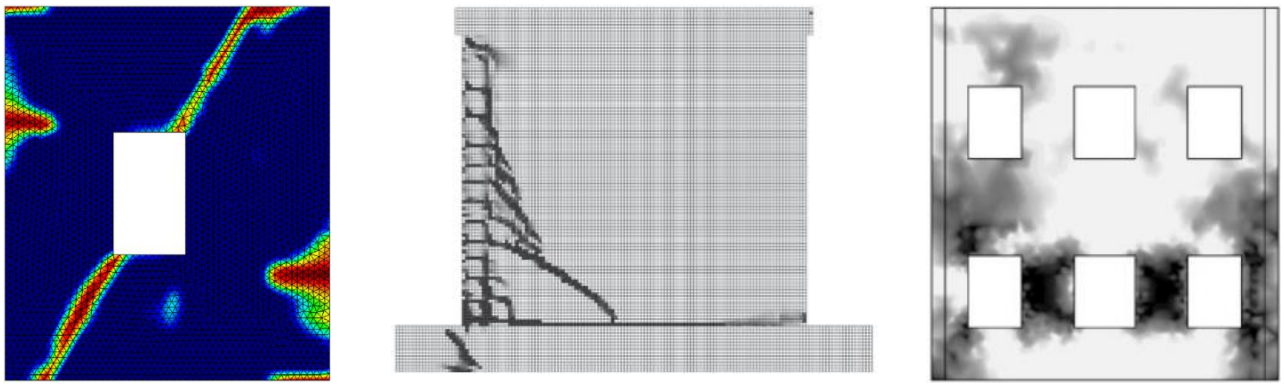

(**a**) (**b**) (**c**)

Figure 16. *Cont.*

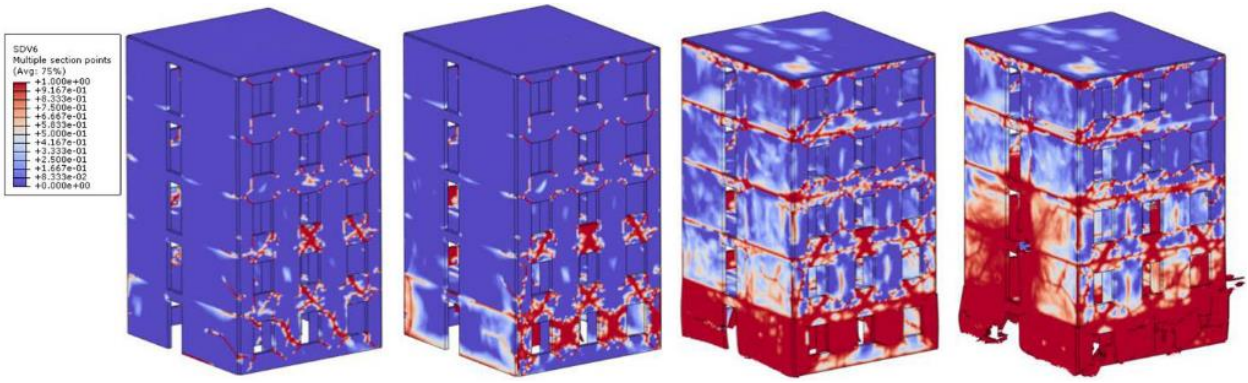

(**d**)

Figure 16. Macro continuum model-based analyses: (**a**) tensile damage for a perforated URM shear wall [170], (**b**) crack pattern for a confined URM shear wall [183], (**c**) damage distribution for a large-scale URM shear wall [169], (**d**) damage distributions of a URM building under sequential ground motions (the plots from to left to right are corresponding to the cases: end of the mainshock, aftershock at 20.75 s, aftershock at 22.50 s, and aftershock at 24.25 s) [187].

The macro element approach intends to idealize masonry systems into several components using structural elements/connectors (e.g., spring, hinge, interface, truss, beam, frame). Each component is represented with a phenomenological (e.g., from experimental data) or mechanical-based (e.g., from Euler Bernoulli beam formulation) material response. For instance, masonry shear walls are typically transformed into an assemblage of piers (i.e., principal vertical resistant elements to both dead and seismic forces), spandrels (i.e., secondary elements that couple piers), and diagonal connecting elements (i.e., shear crack elements) [188–198], as illustrated in Figure 17. At the building level, masonry buildings are discretized into several panel-scale deformable structural components (e.g., piers or spandrels) and/or rigid bodies (representing masonry portions that experience no/limited damage) [199–209]. The macro element strategy might be the most widely used approach for large-scale masonry structural analysis, particularly for the seismic assessment at the building level due to its superior computational efficiency, compared to both micro and macro continuum models.

4.2.1. Unreinforced Masonry Shear Walls and Buildings

Macro continuum models were initially developed for URM structures, focusing on predicting the peak strength (i.e., failure envelope). The first group of available studies involves only the investigation of monotonic behaviors for URM shear walls, such as [170,176,178–180,182]. The primary objective is to validate the capability of macro continuum models to predict the peak strength, while ductility, stiffness degradation, and post-peak behavior received less attention due to the inadequacy of monotonic-based models.

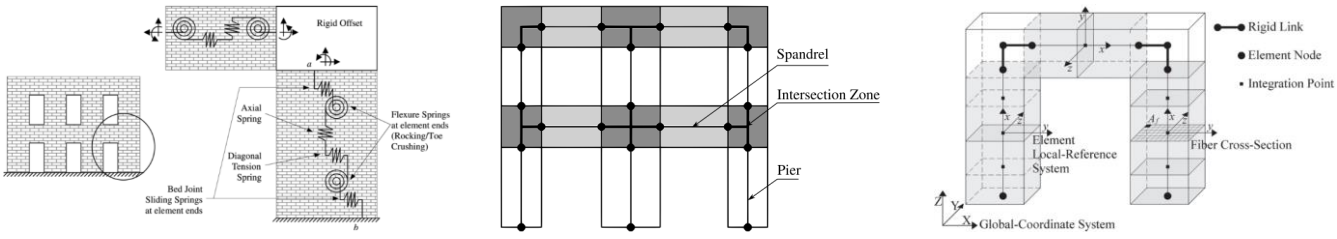

(**a**) (**b**) (**c**)

Figure 17. *Cont.*

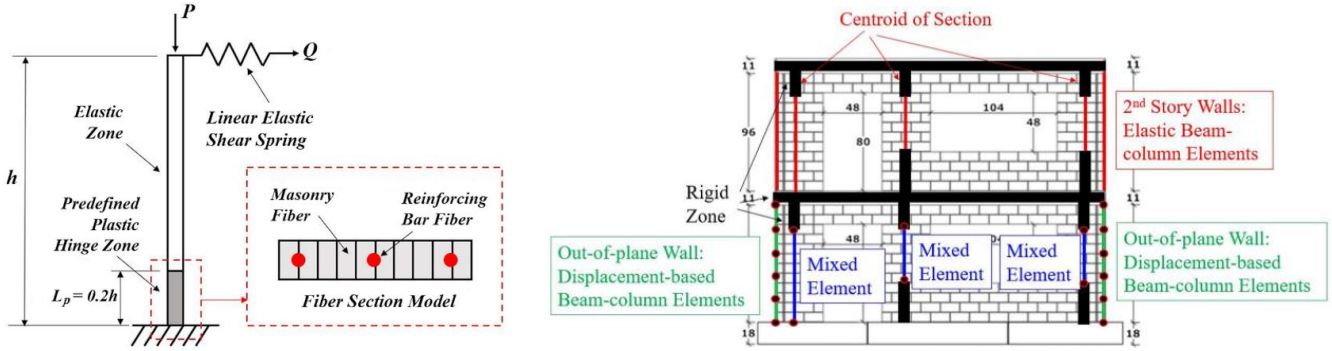

Figure 17. Macro-element-based discretization schemes for (**a**–**c**) URM shear walls/buildings [189,194,209] and (**d**,**e**) RM shear walls/buildings [196,210].

With the increasing availability of experimental data about the hysteretic behavior of masonry materials, more advanced macro continuum models were developed [169,171,174,175,184–186], which were employed for the hysteretic behavior predictions of URM shear walls. For instance, two URM shear walls with different height-to-width ratios, tested in [37], were widely used as validation cases. In the test program [37], the first wall had a height-to-width ratio of 2.00, exhibiting a flexural failure mode, as shown in Figure 18a. Experimental hysteretic behavior indicated a nonlinear response with limited energy dissipation and significant ductility, which was reasonably predicted in the relevant studies [175,184,185], as shown in Figure 18b–d. The second URM shear wall is squatter, with a height-to-width ratio of 1.25, governed by shear failure, characterized by an abrupt strength degradation and a larger energy dissipation compared to the flexural-governed wall shown in Figure 19. Although with some discrepancies, the macro continuum models [175,184,185] can describe the main characteristics of shear-dominated URM shear walls. However, the limitations in representing the crack pattern of macro continuum models are evident since damage initiation and propagation are assumed to be smeared in such models, while the failure of masonry is typically characterized by localized discrete cracks. In order to address this issue, Saloustros et al. [211] refined the macro continuum model with a local crack-tracking algorithm to better describe the localized tensile crack propagation in masonry. The proposed model was proven capable of efficiently capturing the multiple flexural and shear failure modes of a large scale URM shear wall.

In addition to macro continuum models, macro element models have wider applicability in practice-oriented assessments for URM shear walls. Examples include monotonic behavior estimation with a primary interest in the initial stiffness and peak strength [188,191,193,194,198,212,213], and cyclic response assessment focusing on more structural characteristics (e.g., stiffness degradation, energy dissipation capability) [195,202,203,205,206,214]. Based on the assumption that damage could be approximatively concentrated in particular sections of the structure, macro elements can be modeled through lumped plasticity behaviors at specified locations (e.g., at the end and/or midpoint of structural elements). Due to the oversimplification in the idealization of masonry walls or buildings, the crack location and damage distribution cannot be generally obtained explicitly but can be qualitatively estimated through the violation of plastic material laws (e.g., flexural or shear strength).

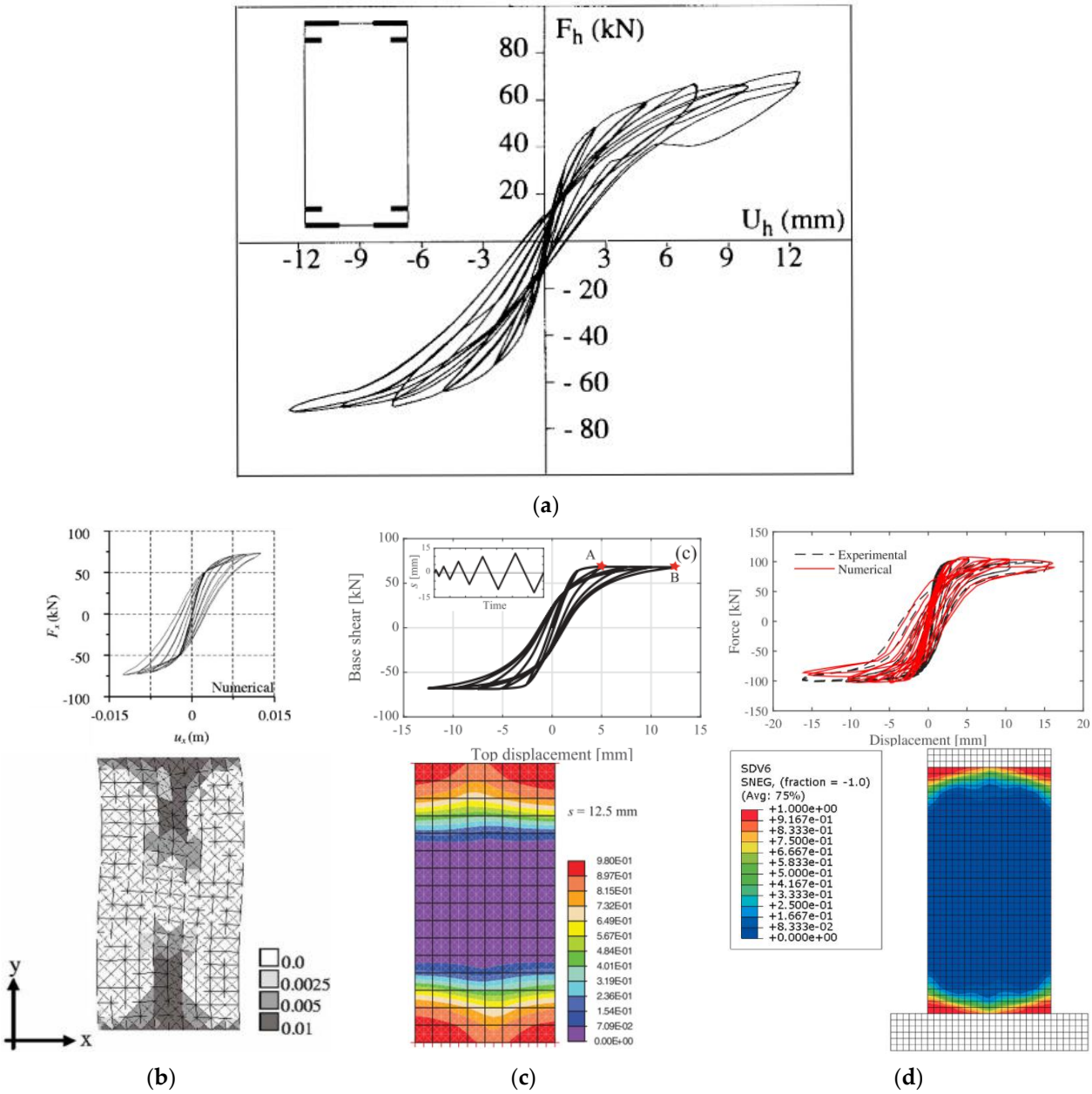

Figure 18. (**a**) Hysteretic behavior and crack pattern of shear-governed URM shear walls from the experimental test [37], and (**b**–**d**) numerical predictions based on the macro continuum models [175,184,185].

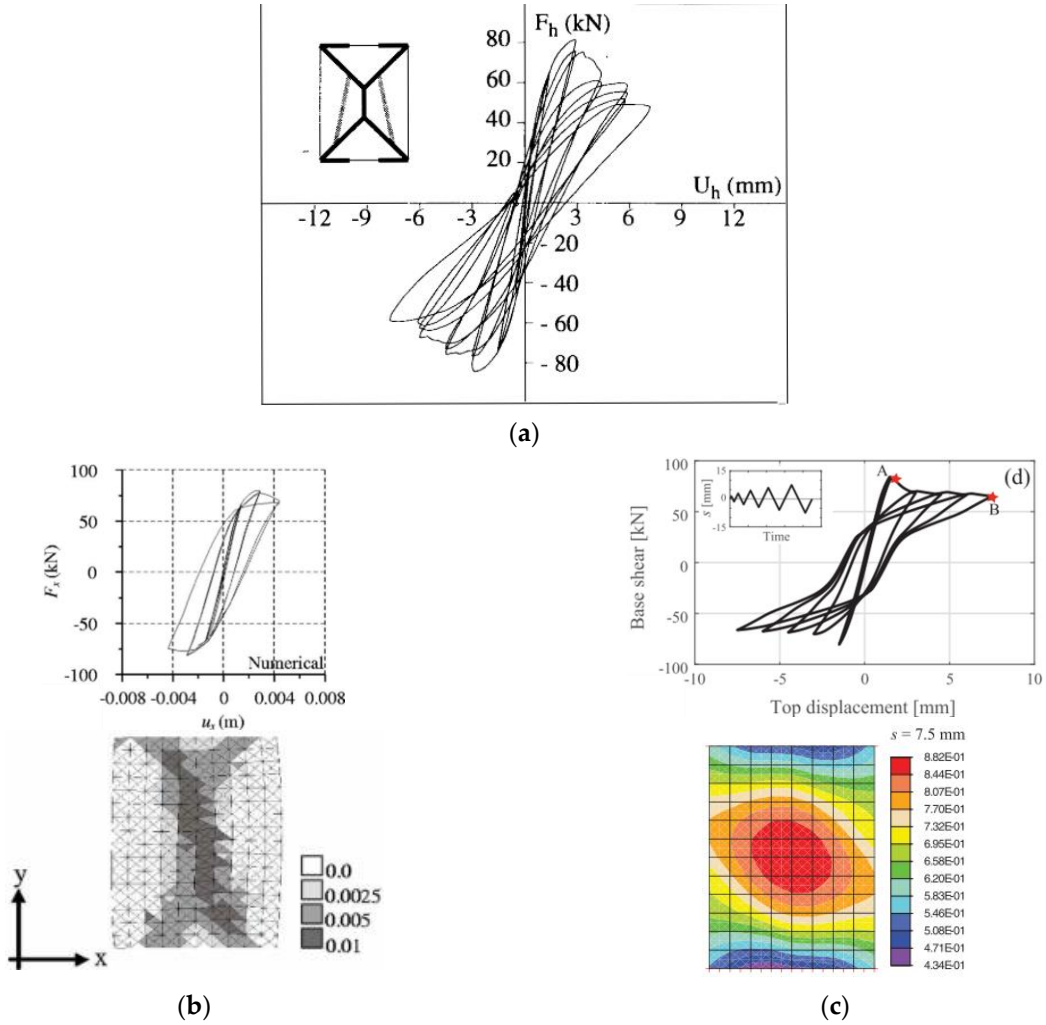

Figure 19. (**a**) Hysteretic behavior and crack pattern of flexural-governed URM shear walls from experimental tests [37], and (**b**,**c**) numerical predictions based on the macro continuum models [175,185].

Owing to its superior computational efficiency, the macro element model is the most widely diffused approach for the seismic behavior assessment of large-scale masonry buildings, as seen in a wide range of available studies [203,205–207,209,215–223]. Rinaldin et al. [203] proposed a generative method for the modeling of perforated walls (i.e., walls with windows or doors), where nonlinear springs were placed at the two ends of masonry elements for describing the flexural behavior and in the middle for representing the response in shear. The proposed macro element modeling strategy was validated against a single pier and a spandrel under cyclic loading, while the building-level performance assessment was conducted in an incremental dynamic analysis framework. However, it was shown that the failure modes of some piers, e.g., PD2 pier shown in Figure 20a,b, were not consistent with the experimental ones. Bracchi and Penna [205,206] made an effort by taking into account second-order effects and developing a more refined flexural stiffness calculation strategy, which is particularly important for building with flexible diaphragms involving large deformation under seismic effects. The validation results, illustrated in Figure 20c, in terms of the failure mechanisms showed the outperformance of the proposed models compared to an existing macro element model [202].

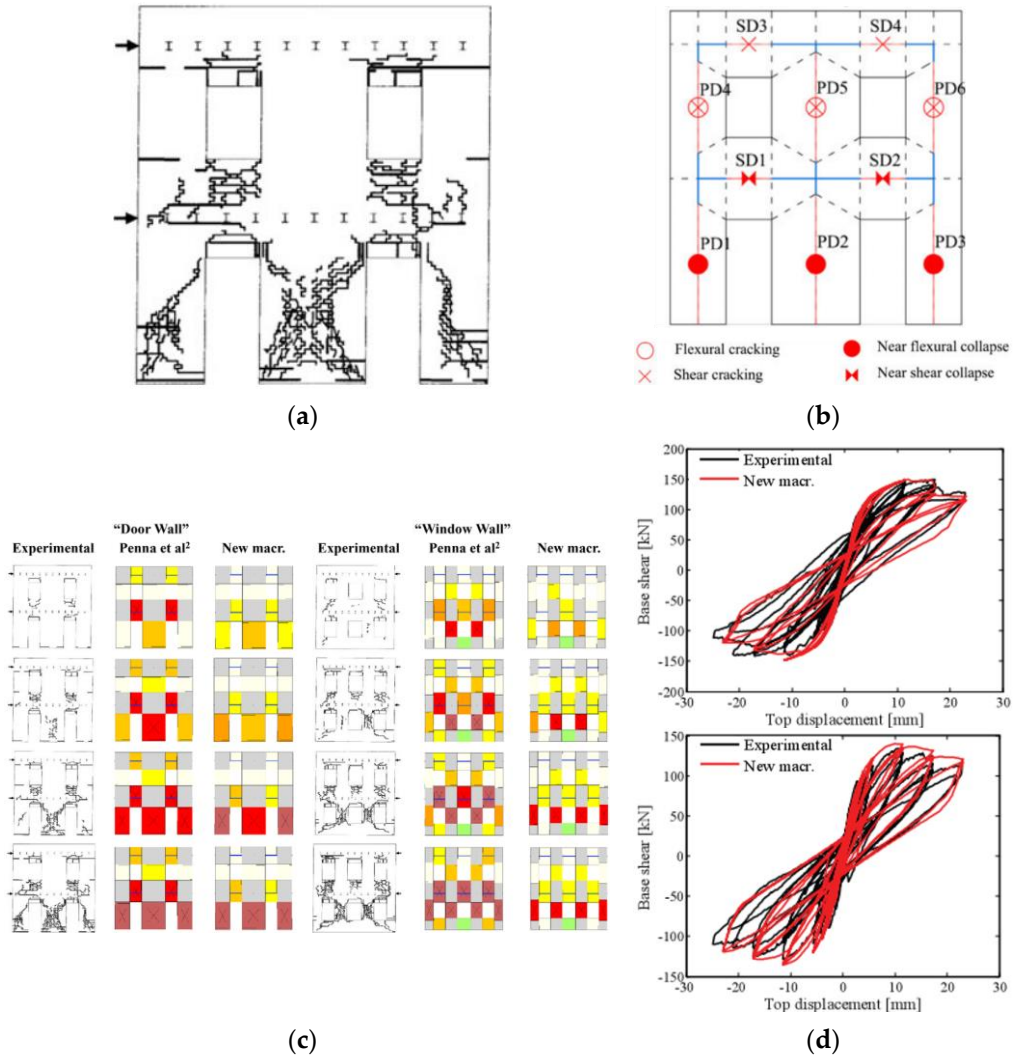

Figure 20. (**a**,**b**) Numerical–experimental comparison in terms of the failure modes of URM buildings [203] and (**c**,**d**) numerical–experimental comparison in terms of the failure modes and hysteretic behaviors of URM buildings [205].

Shabani and Kioumarsi [207] employed a similar structural idealization scheme as that in [203], using a Double Modified Multiple Vertical Line Element Method (DM-MVELM) for the modeling of large-scale URM structures. The main advantage of the proposed model is the consideration of axial–flexural (N-M) interaction, enabling a feasible description of the composite failure mechanism (e.g., combined flexural–shear failure mode) and providing a higher accuracy in terms of the hysteretic behavior compared with other available models. However, these previously discussed models neglected the out-of-plane behavior and thus failed to capture the out-of-plane deformation. Vanin et al. [195] considered the coupled in-plane and out-of-plane effects to propose a three-dimensional macro element formulation, validated against URM walls under static/dynamic in-plane and out-of-plane loading conditions. The proposed macro element model exhibited great potential in predicting the complex failure mode of URM buildings, e.g., cracks are concentrated at the building corner, although the applicability of proposed model at the building level has not yet been examined.

In recent years, a series of comparative studies were performed to evaluate the reliability of macro continuum and macro element models in the seismic performance assessment of URM shear walls and buildings [208,224–226]. Parisse et al. [208] evaluated the influence of modeling assumptions involved in macro modeling approaches with reference to a benchmark URM shear wall by performing pushover analyses. However, large discrepan-

cies were observed in terms of the secant stiffness values and maximum base shear forces, while both macro models exhibit almost identical ductility predictions, as illustrated in Figure 21a. Cannizzaro et al. [224] performed a push-over analysis regarding a two-story building characterized by rigid horizontal diaphragms and different opening arrangements, using four computational strategies: macro element model, macro continuum model, micro model, and limit analysis. The results showed in Figure 21b exhibited significant scatter between the micro models, which implicitly incorporated the orthotropic nature of the masonry media, and other isotropic modeling strategies performed at the macro-scale. Betti et al. [225] reported a comparison of seismic performance predictions obtained by a macro continuum model and a macro element model, concluding that the macro continuum model was capable of reproducing with good confidence the experimental damages, while the macro element model could predict the collapse load but failed to provide a satisfactory reconstruction of the actual collapse mechanism. In all simulations, the macro element model underestimated shear forces since it provided a more pronounced stiffness decay with respect to the macro continuum model.

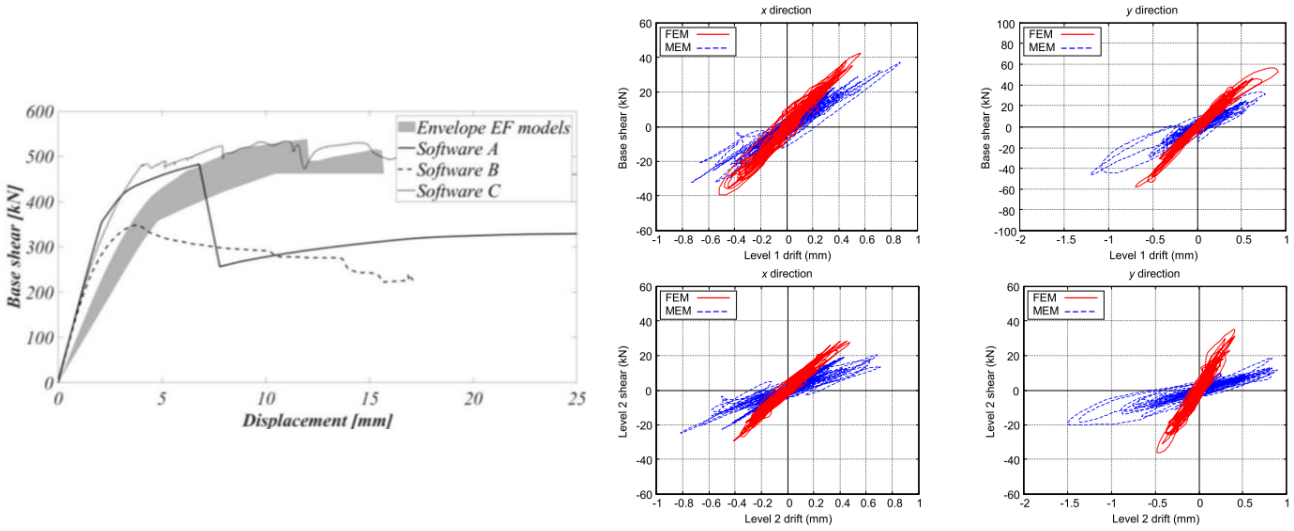

(**a**) (**b**)

Figure 21. Comparison of the base–shear displacement relationship between different modeling strategies (**a**) from [224]: software A (macro element model), software B (macro continuum model), software (micro model), and Envelope of EF models (obtained by macro element models collected from study [216]) and (**b**) from [225]: FEM (macro continuum model) and MEM (macro element model).

Aşıkoğlu et al. [226] performed the nonlinear static pushover analyses for irregular URM buildings using three modeling approaches: the macro continuum model, and beam-based and spring-based macro element models. The results indicated that the results obtained from the macro continuum model closely matched the experimental envelope with an average difference of 4%. However, the macro element model implemented in the software 3DMacro tended to overestimate the peak strength.

4.2.2. Reinforced Masonry Shear Walls and Buildings

Despite the extensive applicability of macro models to URM shear walls and buildings, particularly in the context of historic masonry structures, their potential for modeling RM shear walls and buildings has not been fully explored. Currently, available studies on RM shear walls based on the macro continuum models are limited [177,183,227–229], focusing only on the static monotonic behavior. Furthermore, the effects of reinforcements have not been adequately considered, using either a smeared approach [177] or assuming perfect bonding between the reinforcing bar and block/grout [183,227–229]. Other effects, such as

nonlinear bond slip behavior and dowel effects, are typically neglected, even though these effects have been shown to significantly impact RM shear wall behaviors.

Macro element models have only been introduced to RM shear walls very recently [189,196,210], despite their considerable success in modeling reinforced concrete members. Peruch et al. discussed the applicability of an existing distributed plasticity Timoshenko frame element with fiber cross-sections for the analysis of FGRM shear walls. Cheng and Shing [210] presented a modeling method based on a fiber-section beam-column element idealization to capture the nonlinear in-plane cyclic behavior of flexural-dominated RM walls, with a highlight of considering the buckling and low-cycle fatigue of vertical reinforcing bars using a phenomenological material law. Later, Cheng and Shing [196] developed a more advanced beam-column element capable of capturing the axial–flexural–shear interaction. The proposed model was validated against the tested RM shear walls, and the validation results showed a lower shear strength compared to the test results, but the hysteretic character was reasonably captured. In addition, the developed model was validated against a two-story RM building under seismic loading, as shown in Figure 22. Despite some discrepancies, this efficient macro element model demonstrated its significant potential for the seismic performance assessment of RM buildings.

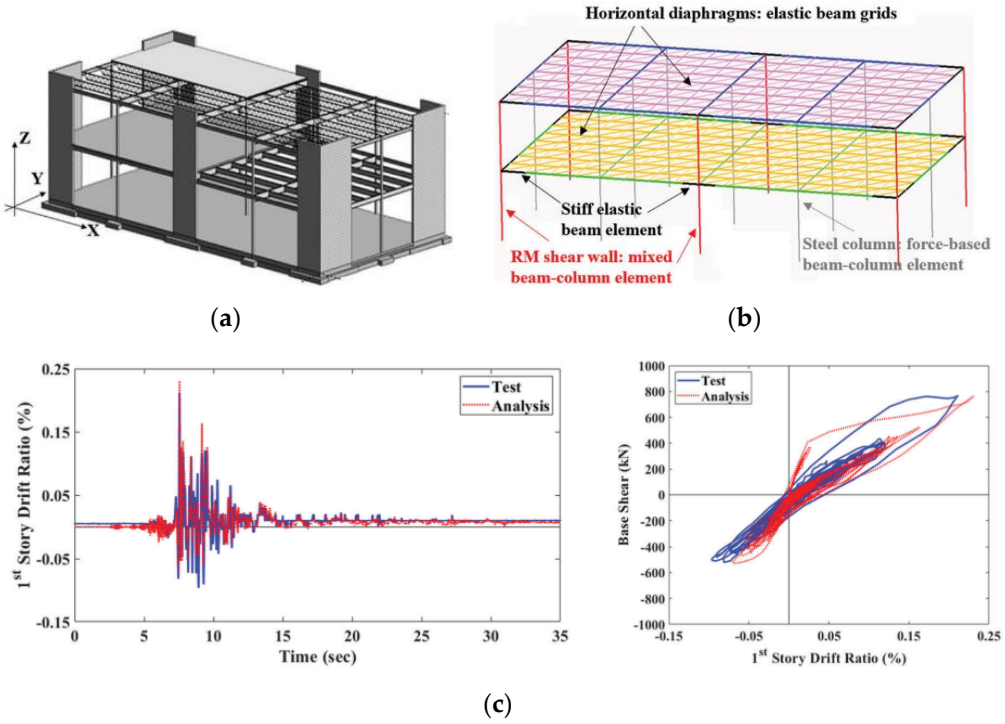

Figure 22. (**a**) Tested building specimen configuration, (**b**) macro element model, and (**c**) experimental–numerical comparison in terms of the time–history drift ratio and base shear–drift ratio relationship [196].

4.3. Future Research Needs

Numerical works that focused on the performance assessment of masonry walls and buildings are reviewed above. Based on the modeling complexity and sophistication level, numerical modeling approaches are divided into micro and macro models.

Micro models have demonstrated significant success in assessing the performance of URM and RM shear walls as reviewed herein, despite their intense computational cost and technical complexity. Nonetheless, future research is necessary to investigate the influence of material parameters on the hysteretic behaviors of URM and RM shear walls using micro models.

Macro models, characterized by numerical efficiency and ease of implementation, are favored by practitioners for more practice-oriented objectives. It can be observed that the

majority of current macro models primarily focused on URM walls and buildings, showing significant impacts on historical masonry structures. Nonetheless, due to the heterogeneity and anisotropy of RM structures, only a few attempts have been made to explore the potential of macro models in assessing the performance of modern RM structures, particularly limited for PGRM walls and buildings. The applicability in evaluating the structural performance of RM walls and buildings (e.g., peak strength, initial/degraded stiffness, deformation capacity, and energy dissipation capability) still remains questionable and requires further study.

The modeling discrepancies between micro and macro models, attributed to the material calibration in some studies, should be paid enough attention. Typically, material determination in the micro and macro continuum models is significantly challenging without relevant experimental information. A reasonable material calibration framework should be developed for this purpose. The well-developed micro and macro continuum models of URM and RM structures are expected to be used further for the validation of efficient macro element models.

It is noteworthy that the numerical and analytical studies at the building level, especially for the RM building, are limited. Factors such as diaphragm stiffness, in-plane and out-of-plane interaction, and coupling of different failure modes should be further investigated to facilitate a more feasible assessment of masonry buildings.

5. Fragility and Performance Assessment of Masonry Walls/Buildings

A fundamental prerequisite for implementing PBD is the establishment of damage states corresponding to different performance levels. For instance, Li and Weigel [230] examined the definition of qualitative and quantitative damage states for concrete masonry walls (see Table 3) provided in HAZUS [231] using experimental test data. The analysis results indicated that the HAZUS definitions on the damage states best correlate with high aspect ratio and flexural governed walls, while not being applicable to shear-critical walls. A more refined damage state definition scheme was developed by Murcia-Delso and Shing [232], in which RM walls were distinguished by different failure modes. A total of six damage states were defined qualitatively and quantitatively, as shown in Table 4. Performance assessment of masonry walls and buildings towards these damage indicators is typically achieved through fragility functions, which in this context provide the probability of exceeding a damage state as a function of Engineering Demanding Parameters, i.e., EDPs (e.g., strength, ductility, drift ratio, dissipated energy) [233]. This procedure requires robust experimental information or advanced analytical tools, as discussed previously.

Fragility function can be fully developed based on the experimental data. For example, Ruiz-García and Negrete [234] developed drift-based fragility curves associated with selected damage states (e.g., first diagonal cracking, lateral strength point). The relevant information was obtained by compiling a database composed of 118 tested confined masonry walls. The influence of factors, such as brick-type and amount of horizontal reinforcement, is considered. Araya-Letelier et al. [235] developed fragility functions for PGRM shear walls with bed-joint reinforcement using data from 44 and 32 full-scale in plane cyclic tests conducted on clay brick (CLB) walls and hollow concrete block (HCB) walls, respectively. Two EDPs were used to derive the fragility functions: the story drift ratio and the force-based normalized shear demand parameter, as shown in Figure 23. Lotfy et al. [236] employed the damage state definition presented in Table 4 to develop a series of fragility curves by combining experimental data from 91 tested RM wall specimens. Furthermore, the influence of aspect ratio on the fragility functions for flexurally dominated walls was studied and shown in Figure 24. The discrepancies between fragility curves implied the importance of considering aspect ratio during the fragility analysis.

Table 3. Qualitative and quantitative definition of damage states [231].

Damage States	Qualitative Definition (RM1L/RM2L *)	Quantitative Definition (Drift Ratio)			
		High-Code *	Moderate-Code *	Low-Code *	Pre-Code *
Slight	Diagonal hairline cracks on wall surfaces; large cracks around door and window openings in walls with large proportion of openings; minor separation of walls from the floor and roof diaphragms.	0.0004	0.0004	0.0004	0.0003
Moderate	Most wall surfaces exhibit diagonal cracks; some of the shear walls have exceeded their yield capacities indicated by larger diagonal cracks. Some walls may have visibly pulled away from the roof.	0.0008	0.0007	0.0006	0.0005
Extensive	Most shear walls with large openings have exceeded their yield capacities, and some of the walls have exceeded their ultimate capacities, indicated by large, through-the-wall diagonal cracks and visibly buckled wall reinforcement. Partial collapse of the roof may result from failure of wall to diaphragm connections.	0.024	0.019	0.016	0.013
Complete	Structure has collapsed or is in imminent danger of collapse due to failure of the wall anchorages or the wall panels. Approximately 13% (low-rise) of the total area of the building is expected to be collapsed.	0.070	0.053	0.044	0.035

* RM1L/RM2L is used to denote low-rise reinforced masonry bearing walls, generally ranging from 1-3 stories, with a total height less than 20 feet. * High-code, moderate-code, low-code correspond to the "quality" of the design code to which the building was designed. Pre-code indicates that the building was not designed for seismic loading.

Table 4. Qualitative and quantitative definition of damage states [232].

Damage States	Description of Damage	Identification Criteria to Calibrate Fragility Functions
Slight flexural damage (DS1)	■ A few flexural and shear cracks with hardly noticeable residual crack widths. ■ Slight yielding of extreme vertical reinforcement. ■ No spalling. ■ No fracture or buckling of vertical reinforcement. ■ No structurally significant damage.	When a flexure-critical wall was loaded to 80% of its peak in-plane lateral resistance.
Moderate flexural damage (DS2)	■ Numerous flexural and diagonal cracks. ■ Mild toe crushing with vertical cracks or light spalling at wall toes. ■ No fracture or buckling of reinforcement. ■ Small residual deformation.	When a flexure-critical wall was loaded to its peak in-plane lateral resistance.
Severe flexure damage (DS3)	■ Severe flexural cracks. ■ Severe toe crushing and spalling. ■ Fracture or buckling of vertical reinforcement. ■ Significant residual deformation.	When a flexure-critical wall was loaded beyond its peak resistance and exhibited a load drop of 20% with respect to the peak.
Moderate diagonal shear damage (DS4)	■ First occurrence of major diagonal cracks. ■ Cracks remain closed with hardly noticeable residual crack widths after load removal.	When major diagonal cracks crossing almost the entire length of a wall first occurred, based on experimental observations.
Severe diagonal shear damage (DS5)	■ Wide diagonal cracks with typically one or more cracks in each direction. ■ Crushing or spalling at wall toes.	When a shear-critical wall reached its peak shear resistance.
Severe sliding shear damage (DS6)	■ Large permanent wall offset. ■ Spalling and crushing at the wall toes due to dowel action and flexure. ■ Shear fracture of vertical reinforcement or dowels.	Derived analytically.

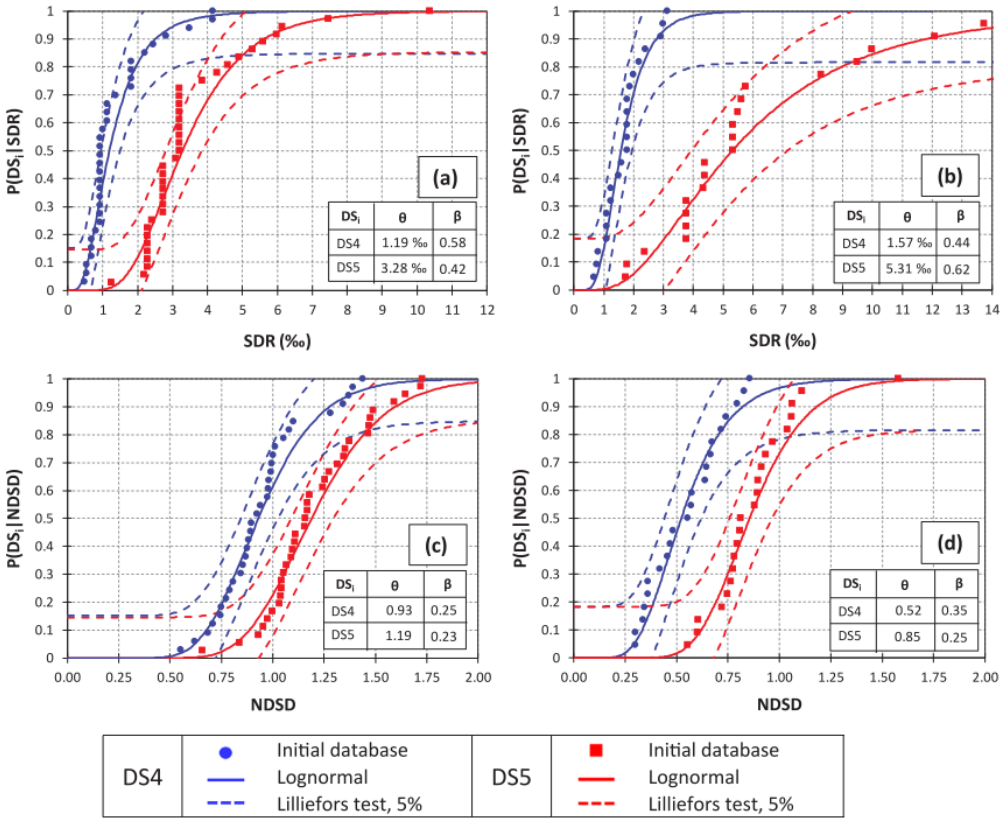

Figure 23. Comparison of fragility functions: (**a**) CLB walls (story drift ratio), (**b**) HCB walls (story drift ratio), (**c**) CLB walls (normalized diagonal shear demand), and (**d**) HCB walls (normalized diagonal shear demand) (from [235]).

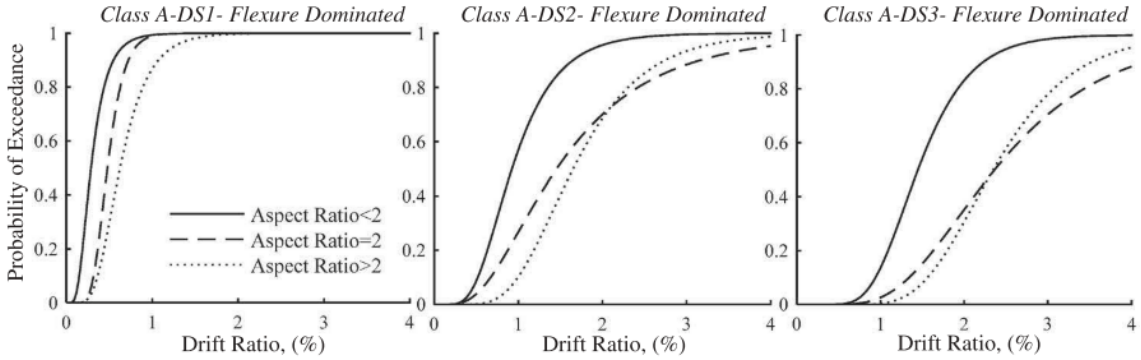

Figure 24. Influence of aspect ratio on the fragility curves (from [236]).

Additional experimentally based fragility curves and performance assessments for masonry walls with different configurations are available in other studies, for example, URM walls [237–239], RM shear walls [232], and RM walls with boundary elements or confined masonry walls [240,241]. With the advancement of damage detection technology, researchers began exploring the application of such technology for crack detection. Asjodi and Dolatshahi [238] introduced a novel methodology for identifying the post-earthquake damage states of URM walls using visual damage features, in which the various types of cracking and crushing areas were measured. The measurement results were further used for the qualitative damage state identification and corresponding fragility function development. Although significant efforts have been devoted to the experimentally based fragility analysis and performance assessment of masonry walls, no studies are available for

the system evaluation, mainly due to the limited experimental data at the masonry building level. As such, more systematic experimental testing and data compilation is highly needed to facilitate the performance-based design and evaluation of masonry buildings. Moreover, a considerable number of seismic retrofitting approaches were developed and implemented (e.g., [242,243]), especially for conventional URM buildings, as illustrated in various studies (e.g., [244,245]). These buildings often adhere to outdated design codes and may experience significant damage under seismic loadings. Given the vulnerability of such structures, it is imperative to apply performance-based evaluation for such existing systems and performance-based design to retrofitted systems with innovative retrofitting approaches, because they may behave differently from conventional building systems. For this purpose, more experimental tests to validate the effectiveness of retrofitting approach and corresponding performance improvements should be conducted.

Conversely, the analytical models were widely used for the performance assessment and corresponding collapse fragility analysis of masonry buildings [246–252]. However, most studies focused on the URM buildings [246,247,249–252], with only one focusing on the modern RM building [248]. Siyam et al. [248] performed the collapse fragility analysis for a ductile RM concrete block wall system using a macro-element model, in which two methods were used to define the collapse: (1) collapse occurs when a certain limit of maximum inter-story drift is exceeded, and (2) collapse occurs when a certain limit of intensity measure is exceeded. Corresponding collapse fragility curves are shown in Figure 25. It can be seen that analytical-based fragility analyses and performance assessments for RM buildings are scarce due to the limited availability of macro models for RM walls and buildings, as reviewed in Section 4. To accomplish performance-based design and evaluation of masonry buildings, more efforts need be devoted to developing practice-oriented macro models that are capable of predicting the overall nonlinear behavior (i.e., not just the strength as in the most existing empirical models) with computational efficiency (i.e., not like micro models widely used for research purposes).

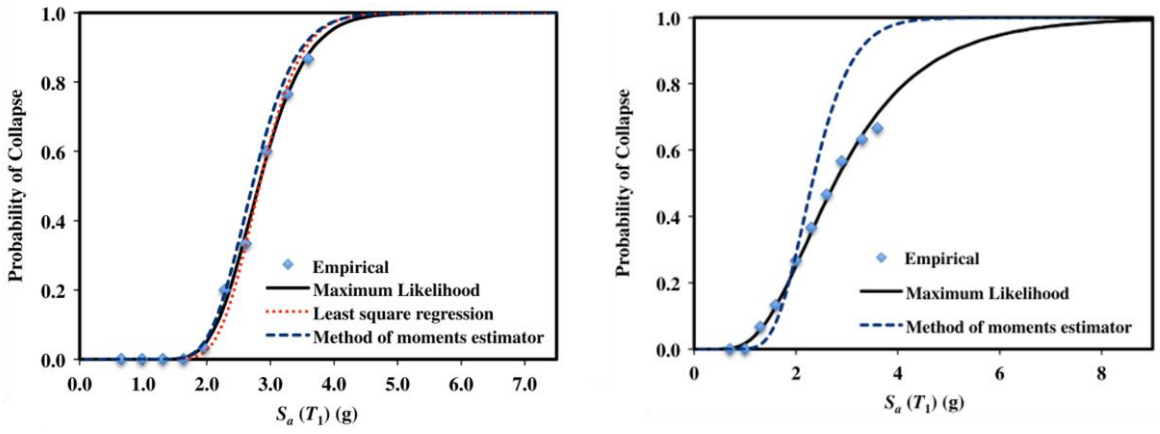

Figure 25. Collapse fragility curves using different fitting methods and collapse defined by (**a**) maximum inter-story drift and (**b**) intensity measure (from [248]).

6. Conclusions

Performance-based design (PBD) is an effective alternative for addressing the shortcomings of conventional prescriptive design codes. The implementation of PBD is essential for achieving improved structural resilience. To facilitate the next-generation PBD for masonry buildings, this paper presents a comprehensive review of experimental and numerical/analytical studies on the performance assessment of both conventional unreinforced and modern reinforced masonry walls and buildings, followed by previous efforts in the literature about fragility and performance assessment of masonry walls or buildings. In addition to strength-based characterizations, this paper places more emphasis

on reviewing performance aspects of masonry walls/buildings in the public literature, such as those related to hysteretic behavior, ductility, energy dissipation capability, and stiffness degradation. These aspects are of critical importance for the implementation of PBD in the masonry community.

Experimental studies play a critical role in generating valuable information that enables a deeper understanding of complex structural performance of masonry buildings. These studies also contribute to the development of analytical models and tools for advancing the knowledge and practice of PBD for masonry buildings. It is found that experimental data at the masonry building level, especially for reinforced masonry buildings, is limited. This highlights the need for further experimental efforts to bridge this gap. In addition, certain characteristic behaviors that are crucial to PBD implementation, such as stiffness degradation, energy dissipation, and post-cracking behavior, have not been extensively quantitatively assessed.

Analytical/numerical studies, including micro and macro model-based works, facilitate the implementation of PBD by providing useful tools for performance assessments and fragility analyses. While significant progress has been made for unreinforced masonry structures in this aspect, research on modern reinforced masonry walls and buildings remains limited, and the applicability of some current approaches is questionable. Computationally intensive micro models have the potential to be a material calibration tool for the purpose of developing new macro models for an efficient estimation purpose, presenting an opportunity for future studies to explore and enhance the existing models or develop new ones.

Author Contributions: Conceptualization, B.Z. and Y.L.; investigation, B.Z. and Y.L.; resources, B.Z. and Y.L.; writing—original draft preparation, B.Z.; writing—review and editing, B.Z. and Y.L.; supervision, Y.L.; funding acquisition, Y.L. All authors have read and agreed to the published version of the manuscript.

Funding: The authors would like to acknowledge the financial support provided by the Natural Sciences and Engineering Research Council (NSERC) of Canada through the Collaborative Research and Development (CRD) Grants (CRDPJ 528050-18).

Data Availability Statement: Data sharing is not applicable to this article.

Conflicts of Interest: The authors declare no conflict of interest.

References

1. Ingham, J.M.; Biggs, D.T.; Moon, L.M. How Did Unreinforced Masonry Buildings Perform in the February 2011 Christchurch Earthquake? *Struct. Eng.* **2011**, *89*, 14–18.
2. Dizhur, D.; Ingham, J.; Moon, L.; Griffith, M.; Schultz, A.; Senaldi, I.; Magenes, G.; Dickie, J.; Lissel, S.; Centeno, J.; et al. Performance of Masonry Buildings and Churches in the 22 February 2011 Christchurch Earthquake. *Bull. N. Z. Soc. Earthq. Eng.* **2011**, *44*, 279–296. [CrossRef]
3. Pacific Earthquake Engineering Center. *Guidelines for Performance-Based Seismic Design of Tall Buildings*; Pacific Earthquake Engineering Research Center, College of Engineering, University of California: Berkeley, CA, USA, 2017.
4. Deb, A.; Zha, A.L.; Caamaño-Withall, Z.A.; Conte, J.P.; Restrepo, J.I. Simplified Risk-Targeted Performance-Based Seismic Design Method for Ordinary Standard Bridges. *J. Bridg. Eng.* **2022**, *27*, 04022089. [CrossRef]
5. Li, Y.; Conte, J.P.; Gill, P.E. Probabilistic Performance-Based Optimum Seismic Design Framework: Illustration and Validation. *Comput. Model. Eng. Sci.* **2019**, *120*, 517–543. [CrossRef]
6. Li, Y.; Conte, J.P. Probabilistic Performance-Based Optimum Design of Seismic Isolation for a California High-Speed Rail Prototype Bridge. *Earthq. Eng. Struct. Dyn.* **2018**, *47*, 497–514. [CrossRef]
7. Braverman, J.; Morante, R. *Evaluation of ASCE 4-16 and AISC 43-18 (Draft) for Use in the Risk-Informed Performance-Based Seismic Design of Nuclear Power Plant Structures, Systems, and Components*; Brookhaven National Lab. (BNL): Upton, NY, USA, 2020; Volume 18, ISBN 2207222020.
8. *CSA S304-14*; Design of Masonry Structures. Canadian Standards Association: Mississauga, ON, Canada, 2014.
9. Masonry Society. *Building Code Requirements and Specification for Masonry Structures (TMS 402/602-16)*; The Masonry Society: Boulder, CO, USA, 2016.
10. National Research Council of Canada. *National Building Code of Canada*; NRCC: Ottawa, ON, USA, 2015.

11. NIST. *Research Required to Support Full Implementation of Performance-Based Seismic Design*; National Institute of Standards and Technology: Gaithersburg, MD, USA; U.S. Department of Commerce: Washington, DC, USA, 2009.
12. Hwang, S.H.; Kim, S.; Yang, K.H. In-Plane Lateral Load Transfer Capacity of Unreinforced Masonry Walls Considering Presence of Openings. *J. Build. Eng.* **2022**, *47*, 103868. [CrossRef]
13. Applied Technology Council. *NEHRP Guidelines for the Seismic Rehabilitation of Buildings*; FEMA 273; Federal Emergency Management Agency: Washington, DC, USA, 1997; p. 435.
14. Haach, V.G.; Vasconcelos, G.; Lourenço, P.B. Proposal of a Design Model for Masonry Walls Subjected to In-Plane Loading. *J. Struct. Eng.* **2013**, *139*, 537–547. [CrossRef]
15. CEN (European Committee for Standardization). *Design of Masonry Structures—Part 1-1: General Rules for Reinforced and Unreinforced Masonry Structures*; EN 1996-1-1; Eurocode 6; CEN: Brussels, Belgium, 2012.
16. Izquierdo, K. Statistical Prediction Methods for the In-Plane Shear Strength of Partially Grouted Masonry Walls. Master's Thesis, University of Alberta, Edmonton, AB, Canada, 2021.
17. Abrams, D.P. Performance-Based Engineeringconcepts for Unreinforced Masonry Building Structures. *Prog. Struct. Eng. Mater.* **2001**, *3*, 48–56. [CrossRef]
18. Heerema, P.; Ashour, A.; Shedid, M.; El-Dakhakhni, W. System-Level Displacement- and Performance-Based Seismic Design Parameter Quantifications for an Asymmetrical Reinforced Concrete Masonry Building. *J. Struct. Eng.* **2015**, *141*, 04015032. [CrossRef]
19. Celano, T.; Argiento, L.U.; Ceroni, F.; Casapulla, C. Literature Review of the In-Plane Behavior of Masonry Walls: Theoretical vs. Experimental Results. *Materials* **2021**, *14*, 3063. [CrossRef]
20. Shabani, A.; Kioumarsi, M.; Zucconi, M. State of the Art of Simplified Analytical Methods for Seismic Vulnerability Assessment of Unreinforced Masonry Buildings. *Eng. Struct.* **2021**, *239*, 112280. [CrossRef]
21. D'Altri, A.M.; Sarhosis, V.; Milani, G.; Rots, J.; Cattari, S.; Lagomarsino, S.; Sacco, E.; Tralli, A.; Castellazzi, G.; de Miranda, S. Modeling Strategies for the Computational Analysis of Unreinforced Masonry Structures: Review and Classification. *Arch. Comput. Methods Eng.* **2020**, *27*, 1153–1185. [CrossRef]
22. Cattari, S.; Calderoni, B.; Caliò, I.; Camata, G.; de Miranda, S.; Magenes, G.; Milani, G.; Saetta, A. Nonlinear Modeling of the Seismic Response of Masonry Structures: Critical Review and Open Issues towards Engineering Practice. *Bull. Earthq. Eng.* **2022**, *20*, 1939–1997. [CrossRef]
23. El-Dakhakhni, W.; Ashour, A. Seismic Response of Reinforced-Concrete Masonry Shear-Wall Components and Systems: State of the Art. *J. Struct. Eng.* **2017**, *143*, 03117001. [CrossRef]
24. Vision, S. *Performance Based Seismic Engineering of Buildings*; Structural Engineers Association of California: Sacramento, CA, USA, 1995.
25. *FEMA P-2082*; NEHRP Recommended Seismic Provisions for New Buildings and Other Structures. Building Seismic Safety Council: Washington, DC, USA, 2020.
26. Vaiana, N.; Rosati, L. Classification and Unified Phenomenological Modeling of Complex Uniaxial Rate-Independent Hysteretic Responses. *Mech. Syst. Signal. Process.* **2023**, *182*, 109539. [CrossRef]
27. Vaiana, N.; Capuano, R.; Rosati, L. Evaluation of Path-Dependent Work and Internal Energy Change for Hysteretic Mechanical Systems. *Mech. Syst. Signal Process.* **2023**, *186*, 109862. [CrossRef]
28. Ciampoli, M.; Petrini, F.; Augusti, G. Performance-Based Wind Engineering: Towards a General Procedure. *Struct. Saf.* **2011**, *33*, 367–378. [CrossRef]
29. Dawson, R.; Hall, J.; Davis, J. Performance-Based Management of Flood Defence Systems. In *Proceedings of the Institution of Civil Engineers: Water Management*; Thomas Telford Ltd.: London, UK, 2004; Volume 157, pp. 35–44.
30. Wang, Y.; Burgess, I.; Wald, F.; Gillie, M. *Performance-Based Fire Engineering of Structures*; CRC Press: Boca Raton, FL, USA, 2012; ISBN 9780203868713.
31. Quiel, S.E.; Marjanishvili, S.M.; Katz, B.P. Performance-Based Framework for Quantifying Structural Resilience to Blast-Induced Damage. *J. Struct. Eng.* **2016**, *142*, C4015004. [CrossRef]
32. Hao, H.; Bi, K.; Chen, W.; Pham, T.M.; Li, J. Towards next Generation Design of Sustainable, Durable, Multi-Hazard Resistant, Resilient, and Smart Civil Engineering Structures. *Eng. Struct.* **2023**, *277*, 115477. [CrossRef]
33. Howlader, M.K. In-Plane Behaviour of Unreinforced Masonry (URM) Walls with Openings in Australian Heritage Construction. Ph.D. Thesis, The University of Newcastle, Newcastle, Australia, 2020.
34. Salmanpour, A.H. Displacement Capacity of Structural Masonry. Ph.D. Thesis, ETH Zurich, Zürich, Switzerland, 2017.
35. Abrams, D.P.; Shah, N. *Cyclic Load Testing of Unreinforced Masonry Walls*; Advanced Construction Technology Center Report, No. 92-26-10; University of Illinois at Urbana Champaign: Champaign, IL, USA, 1992.
36. Raijmakers, T.M.J. *Deformation Controlled Tests in Masonry Shear Walls: Report B-92-1156*; TNO-Bouw: Delft, The Netherlands, 1992.
37. Anthoine, A.; Magonette, G.; Magenes, G. Shear-Compression Testing and Analysis of Brick Masonry Walls. In Proceedings of the Proceedings of the 10th European Conference on Earthquake Engineering, Vienna, Austria, 28 August–2 September 1994.
38. Churilov, S.; Dumova-Jovanoska, E. In-Plane Shear Behaviour of Unreinforced and Jacketed Brick Masonry Walls. *Soil Dyn. Earthq. Eng.* **2013**, *50*, 85–105. [CrossRef]
39. Marzaleh, A.S. Seismic In-Plane Behavior of Post-Tensioned Existing Clay Brick Masonry Walls. Ph.D. Thesis, ETH Zurich, Zürich, Switzerland, 2015.

40. Allen, C.; Masia, M.J.; Page, A.W.; Griffith, M.C.; Derakhshan, H.; Mojsilović, N. Experimental Testing of Unreinforced Masonry Walls with Openings Subject to Cyclic In-Plane Shear. In *Brick and Block Masonry-Trends, Innovations and Challenges, Proceedings of the 16th International Brick and Block Masonry Conference (IBMAC 2016), Padova, Italy, 26–30 June 2016*; CRC Press: Boca Raton, FL, USA; pp. 26–30.
41. Messali, F.; Esposito, R.; Ravenshorst, G.J.P.; Rots, J.G. Experimental Investigation of the In-Plane Cyclic Behaviour of Calcium Silicate Brick Masonry Walls. *Bull. Earthq. Eng.* **2020**, *18*, 3963–3994. [CrossRef]
42. Howlader, M.K.; Masia, M.J.; Griffith, M.C. In-Plane Response of Perforated Unreinforced Masonry Walls under Cyclic Loading: Experimental Study. *J. Struct. Eng.* **2020**, *146*, 04020106. [CrossRef]
43. Choudhury, T.; Milani, G.; Kaushik, H.B. Experimental and Numerical Analyses of Unreinforced Masonry Wall Components and Building. *Constr. Build. Mater.* **2020**, *257*, 119599. [CrossRef]
44. Saito, T.; Moya, L.; Fajardo, C.; Morita, K. Experimental Study on Dynamic Behavior of Unreinforced Masonry Walls. *J. Disaster Res.* **2013**, *8*, 305–311. [CrossRef]
45. Da Porto, F. In-Plane Cyclic Behaviour of Thin Layer Joint Masonry Walls. Ph.D. Thesis, Universita' Degli Studi di Trento, Trento, Italy, 2005.
46. Magenes, G.; Morandi, P.; Penna, A. *D 7.1c Test Results on the Behaviour of Masonry under Static Cyclic in Plane Lateral Loads*; University of Pavia: Agropoli, Italy, 2008.
47. Petry, S.; Beyer, K. Cyclic Test Data of Six Unreinforced Masonry Walls with Different Boundary Conditions. *Earthq. Spectra* **2015**, *31*, 2459–2484. [CrossRef]
48. Salmanpour, A.H.; Mojsilović, N.; Schwartz, J. Displacement Capacity of Contemporary Unreinforced Masonry Walls: An Experimental Study. *Eng. Struct.* **2015**, *89*, 1–16. [CrossRef]
49. Magenes, G.; Penna, A.; Galasco, A.; da Paré, M. In-Plane Cyclic Shear Tests of Undressed Double Leaf Stone Masonry Panels. In Proceedings of the 8th International Masorny Conference, Dresden, Germany, 4–7 July 2010.
50. Wallace, M. What TCCMAR Taught Us. *Mag. Mason. Constr.* **1998**, *11*, 523–529.
51. Shing, P.B.; Schuller, M.; Hoskere, V.S. In-Plane Resistance of Reinforced Masonry Shear Walls. *J. Struct. Eng.* **1990**, *116*, 619–640. [CrossRef]
52. Shing, B.P.B.; Member, A.; Noland, J.L.; Klamerus, E.; Spaeh, H. Inelastic Behaviors of Concrete Masonry Shear Walls. *J. Struct. Eng.* **1990**, *115*, 2204–2225. [CrossRef]
53. Takashi, K.; Hiroshi, I.; Yoshiharu, Y.; Ryogo, K. Seismic Capacity of Reinforced Masonry Walls Including Effects of Axial Stress. In Proceedings of the 4th Canadian Masonry Symposium, Fredericton, NB, USA, 2–4 June 1986; pp. 163–174.
54. Kaminosono, T.; Teshigawara, M.; Haraishi, H.; Fujiissawa, M.; Nakaoka, A. Expermental Study on Seismic Performance of Reinforced Masonry Walls. In Proceedings of the Ninth World Conference on Earthquake Engineering, Tokyo, Japan, 2–9 August 1988; pp. VI-109–VI-114.
55. Matsumura, A. Effect of Shear Reinforcement in Concrete Masonry Walls. In *Proceedings of the First Joint Technical Coordinating Committee on Masonry Research*; U.S.-Japan Coordinated Earthquake Research Program: Gaitherburg, MD, USA, 1985; p. 9.
56. Shing, P.B.; Schuller, M.; Houskere, V.S.; Carter, E. Flexural and Shear Response of Reinforced Masonry Walls. *Struct. J.* **1990**, *87*, 646–656.
57. Shing, P.B.; Schuller, M.H.; Hoskere, V.S. Strength and Ductility of Reinforced Masonry Shear Walls. In Proceedings of the 5th North American Masonry Conference, Boulder, CO, USA, 3–6 June 1990; pp. 3–6.
58. Shing, P.B.; Klamerus, E.; Spaeh, H.; Noland, J.L. Seismic Performance of Reinforced Masonry Shear Walls. In Proceedings of the 9th World Conference on Earthquake Engineering, Tokyo, Japan, 2–9 August 1988; Volume 6, pp. 103–108.
59. Matsumura, A. Shear Strength of Reinforced Hollow Unit Masonry Walls. In Proceedings of the 4th North American Masonry Conference, Los Angeles, CA, USA, 16–19 August 1987; pp. 50–51.
60. Okamoto, S.; Yamazaki, Y.; Kaminosorno, T.; Teshigawara, M.; Hirashi, H. Seismic Capacity of Reinforced Masonry Walls and Beams. In Proceedings of the 18th Joint Meeting of the U.S. Japan Cooperative Programs in Natural Resource Panel on Wind and Seismic Effects, Gaithersburg, MD, USA, 20–21 February 1987; pp. 307–319.
61. Masonry Standards Joint Committee; American Concrete Institute; Structural Engineering Institute; Masonry Society (U.S.). *Building Code Requirements and Specification for Masonry Structures*; The Masonry Society: Longmont, CO, USA, 2013; ISBN 9781929081431.
62. *AIJ Standards for Structural Design of Masonry Structures (1989 Edition)*; Architectural Institute of Japan: Tokyo, Japan, 1993.
63. Kikuchi, K.; Yoshimura, K.; Yoshida, K.; Tanaka, A.; Urasaki, H.; Kijima, Y.; Mizumasa, N. Experimental Study on Seismic Capacity of Reinforced Fully Grouted Concrete Masonry Walls. In Proceedings of the 13th World Conference on Earthquake Engineering, Vancouver, BC, Canada, 1–6 August 2004; p. 15.
64. Shedid, M.M.T. Ductility of Reinforced Concrete Masonry Shear Walls. Master's Thesis, McMaster University, Hamilton, ON, Canada, 2006.
65. Shedid, M.T.; El-Dakhakhni, W.W.; Drysdale, R.G. Behavior of Fully Grouted Reinforced Concrete Masonry Shear Walls Failing in Flexure: Experimental Results. *J. Struct. Eng.* **2008**, *134*, 1754–1767. [CrossRef]
66. Shedid, M.T. Strategies to Enhance Seismic Performance of Reinforced Masonry Shear Walls. Ph.D. Thesis, McMaster University, Hamilton, ON, Canada, 2009.

67. Voon, K.C.; Ingham, J.M. Experimental In-Plane Strength Investigation of Reinforced Concrete Masonry Walls. *J. Struct. Eng.* **2006**, *132*, 400–408. [CrossRef]
68. Koutalan, F.A. Displacement-Based Seismic Design and Tools for Reinforced Masonry Shear-Wall Structures. Ph.D. Thesis, The University of Texas at Austin, Austin, TX, USA, 2012.
69. Sherman, J.D. Effects of Key Parameters on the Performance of Concrete Masonry Shear Walls under In-Plane Loading. Master's Thesis, Washington State University, Pullman, WA, USA, 2011.
70. Kapoi, C.M. Experimental Performance of Concrete Masonry Shear Walls under In-Plane Loading. Master's Thesis, Washington State University, Pullman, WA, USA, 2012.
71. Hernandez, J.F. Quasi-Static Testing of Cantilever Masonry Shear Wall Segments. Master's Thesis, The University of Texas at Austin, Austin, TX, USA, 2012.
72. Cyrier, W.B. Performance of Concrete Masonry Shear Walls with Integral Confined Concrete Boundary Elements. Master's Thesis, Washington State University, Pullman, WA, USA, 2012.
73. Zhao, Y.; Wang, F. Experimental Studies on Behavior of Fully Grouted Reinforced-Concrete Masonry Shear Walls. *Earthq. Eng. Eng. Vib.* **2015**, *14*, 743–757. [CrossRef]
74. Siyam, M.A.; El-Dakhakhni, W.W.; Shedid, M.T.; Drysdale, R.G. Seismic Response Evaluation of Ductile Reinforced Concrete Block Structural Walls. I: Experimental Results and Force-Based Design Parameters. *J. Perform. Constr. Facil.* **2016**, *30*, 04015066. [CrossRef]
75. Eldin, H.M.S. In-Plane Shear Behaviour of Fully Grouted Reinforced Masonry Shear Wall. Ph.D. Thesis, Concordia University, Montréal, QC, USA, 2016.
76. Seif ElDin, H.M.; Galal, K. In-Plane Seismic Performance of Fully Grouted Reinforced Masonry Shear Walls. *J. Struct. Eng.* **2017**, *143*, 04017054. [CrossRef]
77. Mojiri, S.; El-Dakhakhni, W.W.; Tait, M.J. Shake Table Seismic Performance Assessment of Lightly Reinforced Concrete Block Shear Walls. *J. Struct. Eng.* **2015**, *141*, 04014105. [CrossRef]
78. Mojiri, S.; El-Dakhakhni, W.W.; Tait, M.J. Seismic Fragility Evaluation of Lightly Reinforced Concrete-Block Shear Walls for Probabilistic Risk Assessment. *J. Struct. Eng.* **2015**, *141*, 04014116. [CrossRef]
79. Schultz, A.E. *NIST Research Program on the Seismic Resistance of Partially-Grouted Masonry Shear Walls*; NISTIR 5481; US National Institute of Standards and Technology: Gaithersburg, MD, USA, 1994; p. 110.
80. Schultz, A.E. Seismic Resistance of Partially-Grouted Masonry Shear Walls. In Proceedings of the Eleven World Conference on Earthquake Engineering, Acapulco, Mexico, 23–28 June 1996; pp. 211–222.
81. Maleki, M. Behaviour of Partially Grouted Masonry Shear Walls under Cyclic Reversed Loading. Ph.D. Thesis, McMaster University, Hamilton, ON, Canada, 2008.
82. Hamedzadeh, A. On the Shear Strength of Partially Grouted Concrete Masonry. Master's Thesis, University of Calgary, Calgary, AB, Canada, 2013.
83. Bolhassani, M. Improvement of Seismic Performance of Ordinary Reinforced Partially Grouted Concrete Masonry Shear Walls. Ph.D. Thesis, Drexel University, Philadelphia, PA, USA, 2015.
84. Ramírez, P.; Sandoval, C.; Almazán, J.L. Experimental Study on In-Plane Cyclic Response of Partially Grouted Reinforced Concrete Masonry Shear Walls. *Eng. Struct.* **2016**, *126*, 598–617. [CrossRef]
85. Calderón, S.; Vargas, L.; Sandoval, C.; Araya-Letelier, G. Behavior of Partially Grouted Concrete Masonry Walls under Quasi-Static Cyclic Lateral Loading. *Materials* **2020**, *13*, 2424. [CrossRef]
86. Rizaee, S. Assessing Bond Beam Horizontal Reinforcement Efficacy with Different End Anchorage Conditions in Concrete Block Masonry Shear Walls. Master's Thesis, University of Calgary, Calgary, AB, Canada, 2015.
87. Kasparik, T.; Tait, M.J.; El-Dakhakhni, W.W. Seismic Performance Assessment of Partially Grouted, Nominally Reinforced Concrete-Masonry Structural Walls Using Shake Table Testing. *J. Perform. Constr. Facil.* **2014**, *28*, 216–227. [CrossRef]
88. Elmapruk, J.; ElGawady, M.A.; Hassanli, R. Experimental and Analytical Study on the Shear-Strength of Partially Grouted Masonry Walls. *J. Struct. Eng.* **2020**, *146*, 04020147. [CrossRef]
89. Hidalgo-Leiva, D.A.; Picado-Arguedas, A.; Sánchez-Vargas, N. In-Plane Cyclic Performance of Confined Partially Grouted Masonry Walls with Joint and Vertical Reinforcement. *Eng. Struct.* **2021**, *245*, 112881. [CrossRef]
90. Calderón, S.; Sandoval, C.; Araya-Letelier, G.; Inzunza, E.; Milani, G. Quasi-Static Testing of Concrete Masonry Shear Walls with Different Horizontal Reinforcement Schemes. *J. Build. Eng.* **2021**, *38*, 102201. [CrossRef]
91. Elmapruk, J.H. Shear Strength of Partially Grouted Squat Masonry Shear Walls. Master's Thesis, Washington State University, Pullman, WA, USA, 2010.
92. Nolph, S.M. In-Plane Shear Performance of Partially Grouted Masonry Shear Walls. Master's Thesis, Washington State University, Pullman, WA, USA, 2010.
93. Nolph, S.M.; ElGawady, M.A. Static Cyclic Response of Partially Grouted Masonry Shear Walls. *J. Struct. Eng.* **2012**, *138*, 864–879. [CrossRef]
94. Hoque, N. In-Plane Cyclic Testing of Reinforced Concrete Masonry Walls to Assess the Effect of Varying Reinforcement Anchorage and Boundary Conditions. Master's Thesis, University of Calgary, Calgary, AB, Canada, 2013.
95. Tomaževič, M.; Lutman, M.; Petković, L. Seismic Behavior of Masonry Walls: Experimental Simulation. *J. Struct. Eng.* **1996**, *122*, 1040–1047. [CrossRef]

96. Voon, K.C.; Ingham, J.M. *Shear Strength of Concrete Masonry Walls*; Report No. 611; Department of Civil and Environmental Engineering, University of Auckland: Auckland, New Zealand, 2003.
97. Minaie, E.; Mota, M.; Moon, F.L.; Hamid, A.A. In-Plane Behavior of Partially Grouted Reinforced Concrete Masonry Shear Walls. *J. Struct. Eng.* **2010**, *136*, 1089–1097. [CrossRef]
98. Oan, A. Diagonal Shear of Partially Grouted Concrete Masonry Panels. Ph.D. Thesis, University of Calgary, Calgary, AB, Canada, 2013.
99. Psilla, N.; Tassios, T.P. Design Models of Reinforced Masonry Walls under Monotonic and Cyclic Loading. *Eng. Struct.* **2009**, *31*, 935–945. [CrossRef]
100. Lourenço, P.B.; Avila, L.; Vasconcelos, G.; Alves, J.P.P.; Mendes, N.; Costa, A.C. Experimental Investigation on the Seismic Performance of Masonry Buildings Using Shaking Table Testing. *Bull. Earthq. Eng.* **2013**, *11*, 1157–1190. [CrossRef]
101. Aldemir, A.; Binici, B.; Canbay, E.; Yakut, A. Lateral Load Testing of an Existing Two Story Masonry Building up to near Collapse. *Bull. Earthq. Eng.* **2017**, *15*, 3365–3383. [CrossRef]
102. Yi, T.; Moon, F.L.; Leon, R.T.; Kahn, L.F. Lateral Load Tests on a Two-Story Unreinforced Masonry Building. *J. Struct. Eng.* **2006**, *132*, 643–652. [CrossRef]
103. Paquette, J.; Bruneau, M. Pseudo-Dynamic Testing of Unreinforced Masonry Building with Flexible Diaphragm. *J. Struct. Eng.* **2003**, *6*, 708–716. [CrossRef]
104. Cohen, G.L.; Klingner, R.E.; Hayes, J.R.J.; Sweeney, S.C. *Seismic Response of Low-Rise Masonry Buildings with Flexible Roof Diaphragms*; Report No. SR-01-19; U.S. Army Corps of Engineers Construction Engineering Research Laboratory: Washington, DC, USA, 2002.
105. Cohen, G.L.; Klingner, R.E.; Hayes, J.R.; Sweeney, S.C. Seismic Evaluation of Low-Rise Reinforced Masonry Buildings with Flexible Diaphragms: I. Seismic and Quasi-Static Testing. *Earthq. Spectra* **2004**, *20*, 779–801. [CrossRef]
106. Mendes, N.; Lourenço, P.B.; Campos-Costa, A. Shaking Table Testing of an Existing Masonry Building: Assessment and Improvement of the Seismic Performance. *Earthq. Eng. Struct. Dyn.* **2014**, *43*, 247–266. [CrossRef]
107. Avila, L.; Vasconcelos, G.; Lourenço, P.B. Experimental Seismic Performance Assessment of Asymmetric Masonry Buildings. *Eng. Struct.* **2018**, *155*, 298–314. [CrossRef]
108. Tomazevic, M. Seismic Behavior of Plain- and Reinforced-Masonry Buildings. *J. Struct. Eng.* **1994**, *120*, 323–338. [CrossRef]
109. Mavros, M. Experimental and Numerical Investigation of the Seismic Performance of Reinforced Masonry Structures. Ph.D. Thesis, University of California, San Diego, CA, USA, 2015.
110. Mavros, M.; Ahmadi, F.; Shing, P.B.; Klingner, R.E.; McLean, D.; Stavridis, A. Shake-Table Tests of a Full-Scale Two-Story Shear-Dominated Reinforced Masonry Wall Structure. *J. Struct. Eng.* **2016**, *142*, 04016078. [CrossRef]
111. Stavridis, A.; Ahmadi, F.; Mavros, M.; Shing, P.B.; Klingner, R.E.; McLean, D. Shake-Table Tests of a Full-Scale Three-Story Reinforced Masonry Shear Wall Structure. *J. Struct. Eng.* **2016**, *142*, 04016074. [CrossRef]
112. Koutras, A.A.; Shing, P.B. Seismic Behavior of a Partially Grouted Reinforced Masonry Structure: Shake-Table Testing and Numerical Analyses. *Earthq. Eng. Struct. Dyn.* **2020**, *49*, 1115–1136. [CrossRef]
113. Cheng, J.; Koutras, A.A.; Shing, P.B. Evaluation of Collapse Resistance of Reinforced Masonry Wall Systems by Shake-Table Tests. *Earthq. Eng. Struct. Dyn.* **2021**, *50*, 475–494. [CrossRef]
114. Lourenço, P.B.; Rots, J.; Blaauwendraad, J. Two Approaches for the Analysis of Masonry Structures. *Heron* **1995**, *40*, 313–340.
115. Page, A.W. Finite Element Model for Masonry. *J. Struct. Div.* **1978**, *104*, 1267–1285. [CrossRef]
116. Li, Y.; Zeng, B. Modeling of Masonry Structures Using a New 3D Cohesive Interface Material Model Considering Dilatancy Softening. *Eng. Struct.* **2023**, *277*, 115466. [CrossRef]
117. Lotfi, H.R.; Shing, P.B. Interface Model Applied to Fracture of Masonry Structures. *J. Struct. Eng.* **1994**, *120*, 63–80. [CrossRef]
118. Zhai, C.; Wang, X.; Kong, J.; Li, S.; Xie, L. Numerical Simulation of Masonry-Infilled RC Frames Using XFEM. *J. Struct. Eng.* **2017**, *143*, 04017144. [CrossRef]
119. Koutromanos, I.; Shing, P.B. Cohesive Crack Model to Simulate Cyclic Response of Concrete and Masonry Structures. *ACI Struct. J.* **2012**, *109*, 349–358. [CrossRef]
120. Giambanco, G.; Rizzo, S.; Spallino, R. Numerical Analysis of Masonry Structures via Interface Models. *Comput. Methods Appl. Mech. Eng.* **2001**, *190*, 6493–6511. [CrossRef]
121. Abdulla, K.F.; Cunningham, L.S.; Gillie, M. Simulating Masonry Wall Behaviour Using a Simplified Micro-Model Approach. *Eng. Struct.* **2017**, *151*, 349–365. [CrossRef]
122. Zeng, B.; Li, Y.; Cruz Noguez, C. Modeling and Parameter Importance Investigation for Simulating In-Plane and out-of-Plane Behaviors of Un-Reinforced Masonry Walls. *Eng. Struct.* **2021**, *248*, 113233. [CrossRef]
123. Lourenço, P.B. Computational Strategies for Masonry Structures. Ph.D. Thesis, Delft University of Technology, Delft, The Netherlands, 1996.
124. Lourenço, P.B.; Rots, J.G. Multisurface Interface Model for Analysis of Masonry Structures. *J. Eng. Mech.* **1997**, *123*, 660–668. [CrossRef]
125. Citto, C. Two-Dimentional Interface Model Applied to Masonry Structures. Master's Thesis, University of Bologna, Bologna, Italy, 2008.
126. DaPorto, F.; Guidi, G.; Garbin, E.; Modena, C. In-Plane Behavior of Clay Masonry Walls: Experimental Testing and Finite-Element Modeling. *J. Struct. Eng.* **2010**, *136*, 1379–1392. [CrossRef]

127. Kumar, N.; Amirtham, R.; Pandey, M. Plasticity Based Approach for Failure Modelling of Unreinforced Masonry. *Eng. Struct.* **2014**, *80*, 40–52. [CrossRef]
128. Van Zijl, G.P.A.G. Modeling Masonry Shear-Compression: Role of Dilatancy Highlighted. *J. Eng. Mech.* **2004**, *130*, 1289–1296. [CrossRef]
129. Nazir, S.; Dhanasekar, M. A Non-Linear Interface Element Model for Thin Layer High Adhesive Mortared Masonry. *Comput. Struct.* **2014**, *144*, 23–39. [CrossRef]
130. Aref, A.J.; Dolatshahi, K.M. A Three-Dimensional Cyclic Meso-Scale Numerical Procedure for Simulation of Unreinforced Masonry Structures. *Comput. Struct.* **2013**, *120*, 9–23. [CrossRef]
131. Kumar, N.; Barbato, M. New Constitutive Model for Interface Elements in Finite-Element Modeling of Masonry. *J. Eng. Mech.* **2019**, *145*, 04019022. [CrossRef]
132. Macorini, L.; Izzuddin, B.A. A Non-Linear Interface Element for 3D Mesoscale Analysis of Brick-masonry Structures. *Int. J. Numer. Methods Eng.* **2011**, *85*, 1584–1608. [CrossRef]
133. Dolatshahi, K.M.; Aref, A.J. Two-Dimensional Computational Framework of Meso-Scale Rigid and Line Interface Elements for Masonry Structures. *Eng. Struct.* **2011**, *33*, 3657–3667. [CrossRef]
134. Shadlou, M.; Ahmadi, E.; Kashani, M.M. Micromechanical Modelling of Mortar Joints and Brick-Mortar Interfaces in Masonry Structures: A Review of Recent Developments. *Structures* **2020**, *23*, 831–844. [CrossRef]
135. Anand, S.C.; Yalamanchili, K.K. Three-Dimensional Failure Analysis of Composite Masonry Walls. *J. Struct. Eng.* **1996**, *122*, 1031–1039. [CrossRef]
136. Wambacq, J.; Ulloa, J.; Lombaert, G.; François, S. A Variationally Coupled Phase Field and Interface Model for Fracture in Masonry. *Comput. Struct.* **2022**, *264*, 106744. [CrossRef]
137. Fouchal, F.; Lebon, F.; Titeux, I. Contribution to the Modelling of Interfaces in Masonry Construction. *Constr. Build. Mater.* **2009**, *23*, 2428–2441. [CrossRef]
138. D'Altri, A.M.; de Miranda, S.; Castellazzi, G.; Sarhosis, V. A 3D Detailed Micro-Model for the in-Plane and out-of-Plane Numerical Analysis of Masonry Panels. *Comput. Struct.* **2018**, *206*, 18–30. [CrossRef]
139. Greco, F.; Leonetti, L.; Luciano, R.; Nevone Blasi, P. An Adaptive Multiscale Strategy for the Damage Analysis of Masonry Modeled as a Composite Material. *Compos. Struct.* **2016**, *153*, 972–988. [CrossRef]
140. Vandoren, B.; DeProft, K.; Simone, A.; Sluys, L.J. Mesoscopic Modelling of Masonry Using Weak and Strong Discontinuities. *Comput. Methods Appl. Mech. Eng.* **2013**, *255*, 167–182. [CrossRef]
141. Giambanco, G.; LaMalfa Ribolla, E.; Spada, A. Meshless Meso-Modeling of Masonry in the Computational Homogenization Framework. *Meccanica* **2018**, *53*, 1673–1697. [CrossRef]
142. Drougkas, A.; Roca, P.; Molins, C. Experimental Analysis and Detailed Micro-Modeling of Masonry Walls Subjected to in-Plane Shear. *Eng. Fail. Anal.* **2019**, *95*, 82–95. [CrossRef]
143. Marfia, S.; Sacco, E. Multiscale Damage Contact-Friction Model for Periodic Masonry Walls. *Comput. Methods Appl. Mech. Eng.* **2012**, *205–208*, 189–203. [CrossRef]
144. Xu, C.; Xiangli, C.; Bin, L. Modeling of Influence of Heterogeneity on Mechanical Performance of Unreinforced Masonry Shear Walls. *Constr. Build. Mater.* **2012**, *26*, 90–95. [CrossRef]
145. Chaimoon, K.; Attard, M.M. Modeling of Unreinforced Masonry Walls under Shear and Compression. *Eng. Struct.* **2007**, *29*, 2056–2068. [CrossRef]
146. Berto, L.; Saetta, A.; Scotta, R.; Vitaliani, R. Shear Behaviour of Masonry Panel: Parametric FE Analyses. *Int. J. Solids Struct.* **2004**, *41*, 4383–4405. [CrossRef]
147. Gambarotta, L.; Lagomarsino, S. Damage Models for the Seismic Response of Brick Masonry Shear Walls. Part I: The Mortar Joint Model and Its Applications. *Earthq. Eng. Struct. Dyn.* **1997**, *26*, 423–439. [CrossRef]
148. Nie, Y.; Sheikh, A.; Visintin, P.; Griffith, M. An Interfacial Damage-Plastic Model for the Simulation of Masonry Structures under Monotonic and Cyclic Loadings. *Eng. Fract. Mech.* **2022**, *271*, 108645. [CrossRef]
149. Minga, E.; Macorini, L.; Izzuddin, B.A. A 3D Mesoscale Damage-Plasticity Approach for Masonry Structures under Cyclic Loading. *Meccanica* **2018**, *53*, 1591–1611. [CrossRef]
150. Oliveira, D.V.; Lourenço, P.B. Implementation and Validation of a Constitutive Model for the Cyclic Behaviour of Interface Elements. *Comput. Struct.* **2004**, *82*, 1451–1461. [CrossRef]
151. D'Altri, A.M.; Messali, F.; Rots, J.; Castellazzi, G.; de Miranda, S. A Damaging Block-Based Model for the Analysis of the Cyclic Behaviour of Full-Scale Masonry Structures. *Eng. Fract. Mech.* **2019**, *209*, 423–448. [CrossRef]
152. Yavartanoo, F.; Kang, T.H.-K. Dry-Stack Masonry Wall Modeling Using Finite-Element Method. *J. Struct. Eng.* **2022**, *148*, 04022176. [CrossRef]
153. Nie, Y.; Sheikh, A.; Griffith, M.; Visintin, P. A Damage-Plasticity Based Interface Model for Simulating in-Plane/out-of-Plane Response of Masonry Structural Panels. *Comput. Struct.* **2022**, *260*, 106721. [CrossRef]
154. Xie, Z.; Sousamli, M.; Messali, F.; Rots, J.G. A Sub-Stepping Iterative Constitutive Model for Cyclic Cracking-Crushing-Shearing in Masonry Interface Elements. *Comput. Struct.* **2021**, *257*, 106654. [CrossRef]
155. Chisari, C.; Macorini, L.; Izzuddin, B.A. Mesoscale Modeling of a Masonry Building Subjected to Earthquake Loading. *J. Struct. Eng.* **2021**, *147*, 04020294. [CrossRef]

156. Shing, P.B.; Cao, L. *Analysis of Partially Grouted Masonry Shear Walls*; NIST GCR Report; National Institute of Standards and Technology: Gaithersburg, MD, USA, 1997.
157. Bolhassani, M.; Hamid, A.A.; Moon, F.L. Enhancement of Lateral In-Plane Capacity of Partially Grouted Concrete Masonry Shear Walls. *Eng. Struct.* **2016**, *108*, 59–76. [CrossRef]
158. Lee, J.; Fenves, G.L. Plastic-Damage Model for Cyclic Loading of Concrete Structures. *J. Eng. Mech.* **1998**, *124*, 892–900. [CrossRef]
159. Calderón, S.; Sandoval, C.; Arnau, O. Shear Response of Partially-Grouted Reinforced Masonry Walls with a Central Opening: Testing and Detailed Micro-Modelling. *Mater. Des.* **2017**, *118*, 122–137. [CrossRef]
160. Calderón, S.; Arnau, O.; Sandoval, C. Detailed Micro-Modeling Approach and Solution Strategy for Laterally Loaded Reinforced Masonry Shear Walls. *Eng. Struct.* **2019**, *201*, 109786. [CrossRef]
161. Calderón, S.; Milani, G.; Sandoval, C. Simplified Micro-Modeling of Partially-Grouted Reinforced Masonry Shear Walls with Bed-Joint Reinforcement: Implementation and Validation. *Eng. Struct.* **2021**, *234*, 111987. [CrossRef]
162. Fib. *Fib Model Code for Concrete Structures 2010*; John Wiley & Sons, Inc.: Hoboken, NJ, USA, 2013; pp. 1–402.
163. Calderón, S.; Sandoval, C.; Milani, G.; Arnau, O. Detailed Micro-Modeling of Partially Grouted Reinforced Masonry Shear Walls: Extended Validation and Parametric Study. *Arch. Civ. Mech. Eng.* **2021**, *21*, 94. [CrossRef]
164. Koutras, A. Assessment of the Seismic Behavior of Fully and Partially Grouted Reinforced Masonry Structural Systems through Finite Element Analysis and Shake-Table Testing. Ph.D. Thesis, University of California, San Diego, CA, USA, 2019.
165. Koutras, A.A.; Shing, P.B. Finite-Element Modeling of the Seismic Response of Reinforced Masonry Wall Structures. *Earthq. Eng. Struct. Dyn.* **2021**, *50*, 1125–1146. [CrossRef]
166. Koutras, A.A.; Shing, P.B. Numerical and Experimental Assessment of an Improved Design Detail for Partially Grouted Reinforced Masonry Wall Structures. *J. Struct. Eng.* **2021**, *147*, 04021118. [CrossRef]
167. Elmeligy, O.; Aly, N.; Galal, K. Sensitivity Analysis of the Numerical Simulations of Partially Grouted Reinforced Masonry Shear Walls. *Eng. Struct.* **2021**, *245*, 112876. [CrossRef]
168. Wong, P.S.; Vecchio, F.J.; Trommels, H. *Vector2 & Formworks User's Manual*, 2nd ed.; University of Toronto: Toronto, ON, Canada, 2013.
169. Berto, L.; Saetta, A.; Scotta, R.; Vitaliani, R. An Orthotropic Damage Model for Masonry Structures. *Int. J. Numer. Methods Eng.* **2002**, *55*, 127–157. [CrossRef]
170. Pelà, L.; Cervera, M.; Roca, P. An Orthotropic Damage Model for the Analysis of Masonry Structures. *Constr. Build. Mater.* **2013**, *41*, 957–967. [CrossRef]
171. Gambarotta, L.; Lagomarsino, S. Damage Models for the Seismic Response of Brick Masonry Shear Walls. Part II: The Continuum Model and Its Applications. *Earthq. Eng. Struct. Dyn.* **1997**, *26*, 441–462. [CrossRef]
172. Zucchini, A.; Lourenço, P.B. A Coupled Homogenisation-Damage Model for Masonry Cracking. *Comput. Struct.* **2004**, *82*, 917–929. [CrossRef]
173. Pelà, L.; Cervera, M.; Roca, P. Continuum Damage Model for Orthotropic Materials: Application to Masonry. *Comput. Methods Appl. Mech. Eng.* **2011**, *200*, 917–930. [CrossRef]
174. Karapitta, L.; Mouzakis, H.; Carydis, P. Explicit Finite-Element Analysis for the in-Plane Cyclic Behavior of Unreinforced Masonry Structures. *Earthq. Eng. Struct. Dyn.* **2011**, *40*, 175–193. [CrossRef]
175. Calderini, C.; Lagomarsino, S. Continuum Model for In-Plane Anisotropic Inelastic Behavior of Masonry. *J. Struct. Eng.* **2008**, *134*, 209–220. [CrossRef]
176. Lourenço, P.B. Anisotropic Softening Model for Masonry Plates and Shells. *J. Struct. Eng.* **2000**, *126*, 1008–1016. [CrossRef]
177. Lotfi, H.R.; Shing, P.B. An Appraisal of Smeared Crack Models for Masonry Shear Wall Analysis. *Comput. Struct.* **1991**, *41*, 413–425. [CrossRef]
178. Lourenço, P.B.; De Borst, R.; Rots, J.G. A Plane Stress Softening Plasticity Model for Orthotropic Materials. *Int. J. Numer. Methods Eng.* **1997**, *40*, 4033–4057. [CrossRef]
179. Lourenço, P.B.; Rots, J.G.; Blaauwendraad, J. Continuum Model for Masonry: Parameter Estimation and Validation. *J. Struct. Eng.* **1998**, *124*, 642–652. [CrossRef]
180. De Buhan, P.; De Felice, G. A Homogenization Approach to the Ultimate Strength of Brick Masonry. *J. Mech. Phys. Solids* **1997**, *45*, 1085–1104. [CrossRef]
181. Chisari, C.; Macorini, L.; Izzuddin, B.A. An Anisotropic Plastic-Damage Model for 3D Nonlinear Simulation of Masonry Structures. *Int. J. Numer. Methods Eng.* **2023**, *124*, 1253–1279. [CrossRef]
182. Lopez, J.; Oller, S.; Oñate, E.; Lubliner, J. A Homogeneous Constitutive Model for Masonry. *Int. J. Numer. Methods Eng.* **1999**, *46*, 1651–1671. [CrossRef]
183. Yacila, J.; Camata, G.; Salsavilca, J.; Tarque, N. Pushover Analysis of Confined Masonry Walls Using a 3D Macro-Modelling Approach. *Eng. Struct.* **2019**, *201*, 109731. [CrossRef]
184. Shen, J.; Ren, X.; Zhang, Y.; Chen, J. Slip-Enhanced Plastic-Damage Constitutive Model for Masonry Structures. *Eng. Struct.* **2022**, *254*, 113792. [CrossRef]
185. Gatta, C.; Addessi, D.; Vestroni, F. Static and Dynamic Nonlinear Response of Masonry Walls. *Int. J. Solids Struct.* **2018**, *155*, 291–303. [CrossRef]
186. Biye, W.; Junwu, D.; Wen, B.; Yongqiang, Y. Triaxial Elastoplastic Damage Constitutive Model of Unreinforced Clay Brick Masonry Wall. *Earthq. Eng. Eng. Vib.* **2022**, *22*, 157–172. [CrossRef]

187. Shen, J.; Zhang, Y.; Chen, J. Vulnerability Assessment and Collapse Simulation of Unreinforced Masonry Structures Subjected to Sequential Ground Motions. *Bull. Earthq. Eng.* **2022**, *20*, 8151–8177. [CrossRef]
188. Roca, P.; Molins, C.; Marí, A.R. Strength Capacity of Masonry Wall Structures by the Equivalent Frame Method. *J. Struct. Eng.* **2005**, *131*, 1601–1610. [CrossRef]
189. Peruch, M.; Spacone, E.; Shing, P.B. Cyclic Analyses of Reinforced Concrete Masonry Panels Using a Force-Based Frame Element. *J. Struct. Eng.* **2019**, *145*, 04019063. [CrossRef]
190. Ezzeldin, M.; Wiebe, L.; El-Dakhakhni, W. Seismic Collapse Risk Assessment of Reinforced Masonry Walls with Boundary Elements Using the FEMA P695 Methodology. *J. Struct. Eng.* **2016**, *142*, 04016108. [CrossRef]
191. Addessi, D.; Mastrandrea, A.; Sacco, E. An Equilibrated Macro-Element for Nonlinear Analysis of Masonry Structures. *Eng. Struct.* **2014**, *70*, 82–93. [CrossRef]
192. Xu, H.; Gentilini, C.; Yu, Z.; Wu, H.; Zhao, S. A Unified Model for the Seismic Analysis of Brick Masonry Structures. *Constr. Build. Mater.* **2018**, *184*, 733–751. [CrossRef]
193. Pirsaheb, H.; Javad Moradi, M.; Milani, G. A Multi-Pier MP Procedure for the Non-Linear Analysis of in-Plane Loaded Masonry Walls. *Eng. Struct.* **2020**, *212*, 110534. [CrossRef]
194. Chen, S.Y.; Moon, F.L.; Yi, T. A Macroelement for the Nonlinear Analysis of In-Plane Unreinforced Masonry Piers. *Eng. Struct.* **2008**, *30*, 2242–2252. [CrossRef]
195. Vanin, F.; Penna, A.; Beyer, K. A Three-Dimensional Macroelement for Modelling the in-Plane and out-of-Plane Response of Masonry Walls. *Earthq. Eng. Struct. Dyn.* **2020**, *49*, 1365–1387. [CrossRef]
196. Cheng, J.; Shing, P.B. A Beam-Column Element for Modeling Nonlinear Flexural and Shear Behaviors of Reinforced Masonry Walls. *Earthq. Eng. Struct. Dyn.* **2022**, *51*, 1918–1942. [CrossRef]
197. Bracchi, S.; Mandirola, M.; Rota, M.; Penna, A. A New Macroelement-Based Strategy for Modelling Reinforced Masonry Piers. In *Brick and Block Masonry—From Historical to Sustainable Masonry*; CRC Press: London, UK, 2020; pp. 900–907, ISBN 9780367565862.
198. Kesavan, P.; Menon, A. A Macro-Element with Bidirectional Interaction for Seismic Analysis of Unreinforced Masonry Walls. *Earthq. Eng. Struct. Dyn.* **2023**, *52*, 1740–1761. [CrossRef]
199. Caliò, I.; Marletta, M.; Pantò, B. A New Discrete Element Model for the Evaluation of the Seismic Behaviour of Unreinforced Masonry Buildings. *Eng. Struct.* **2012**, *40*, 327–338. [CrossRef]
200. Foraboschi, P.; Vanin, A. Non-Linear Static Analysis of Masonry Buildings Based on a Strut-and-Tie Modeling. *Soil Dyn. Earthq. Eng.* **2013**, *55*, 44–58. [CrossRef]
201. Vanin, F.; Penna, A.; Beyer, K. Equivalent-Frame Modeling of Two Shaking Table Tests of Masonry Buildings Accounting for Their Out-of-Plane Response. *Front. Built Environ.* **2020**, *6*, 42. [CrossRef]
202. Penna, A.; Lagomarsino, S.; Galasco, A. A Nonlinear Macroelement Model for the Seismic Analysis of Masonry Buildings. *Earthq. Eng. Struct. Dyn.* **2014**, *43*, 159–179. [CrossRef]
203. Rinaldin, G.; Amadio, C.; Macorini, L. A Macro-Model with Nonlinear Springs for Seismic Analysis of URM Buildings. *Earthq. Eng. Struct. Dyn.* **2016**, *45*, 2261–2281. [CrossRef]
204. Demirlioglu, K.; Gonen, S.; Soyoz, S.; Limongelli, M.P. In-Plane Seismic Response Analyses of a Historical Brick Masonry Building Using Equivalent Frame and 3D FEM Modeling Approaches. *Int. J. Archit. Herit.* **2020**, *14*, 238–256. [CrossRef]
205. Bracchi, S.; Penna, A. A Novel Macroelement Model for the Nonlinear Analysis of Masonry Buildings. Part 2: Shear Behavior. *Earthq. Eng. Struct. Dyn.* **2021**, *50*, 2212–2232. [CrossRef]
206. Bracchi, S.; Galasco, A.; Penna, A. A Novel Macroelement Model for the Nonlinear Analysis of Masonry Buildings. Part 1: Axial and Flexural Behavior. *Earthq. Eng. Struct. Dyn.* **2021**, *50*, 2233–2252. [CrossRef]
207. Shabani, A.; Kioumarsi, M. A Novel Macroelement for Seismic Analysis of Unreinforced Masonry Buildings Based on MVLEM in OpenSees. *J. Build. Eng.* **2022**, *49*, 104019. [CrossRef]
208. Parisse, F.; Marques, R.; Cattari, S.; Lourenço, P.B. Finite Element and Equivalent Frame Modeling Approaches for URM Buildings: Implications of Different Assumptions in the Seismic Assessment. *J. Build. Eng.* **2022**, *61*, 105230. [CrossRef]
209. Peruch, M.; Spacone, E.; Camata, G. Nonlinear Analysis of Masonry Structures Using Fiber-Section Line Elements. *Earthq. Eng. Struct. Dyn.* **2019**, *48*, 1345–1364. [CrossRef]
210. Cheng, J.; Shing, P.B. Practical Nonlinear Analysis Methods for Flexure-Dominated Reinforced Masonry Shear Walls. *J. Struct. Eng.* **2022**, *148*, 04022109. [CrossRef]
211. Saloustros, S.; Pelà, L.; Cervera, M.; Roca, P. An Enhanced Finite Element Macro-Model for the Realistic Simulation of Localized Cracks in Masonry Structures: A Large-Scale Application. *Int. J. Archit. Herit.* **2018**, *12*, 432–447. [CrossRef]
212. Addessi, D.; Liberatore, D.; Masiani, R. Force-Based Beam Finite Element (FE) for the Pushover Analysis of Masonry Buildings. *Int. J. Archit. Herit.* **2015**, *9*, 231–243. [CrossRef]
213. Liberatore, D.; Addessi, D. Strength Domains and Return Algorithm for the Lumped Plasticity Equivalent Frame Model of Masonry Structures. *Eng. Struct.* **2015**, *91*, 167–181. [CrossRef]
214. Penelis, G.G. An Efficient Approach for Pushover Analysis of Unreinforced Masonry (URM) Structures. *J. Earthq. Eng.* **2006**, *10*, 359–379. [CrossRef]
215. Aghababaie Mobarake, A.; Khanmohammadi, M.; Mirghaderi, S.R. A New Discrete Macro-Element in an Analytical Platform for Seismic Assessment of Unreinforced Masonry Buildings. *Eng. Struct.* **2017**, *152*, 381–396. [CrossRef]

216. Manzini, C.F.; Ottonelli, D.; Degli Abbati, S.; Marano, C.; Cordasco, E.A. *Modelling the Seismic Response of a 2-Storey URM Benchmark Case Study: Comparison among Different Equivalent Frame Models*; Springer: Dordrecht, The Netherlands, 2022; Volume 20, ISBN 1051802101173.
217. Ottonelli, D.; Manzini, C.F.; Marano, C.; Cordasco, E.A.; Cattari, S. A Comparative Study on a Complex URM Building: Part I—Sensitivity of the Seismic Response to Different Modelling Options in the Equivalent Frame Models. *Bull. Earthq. Eng.* **2022**, *20*, 2115–2158. [CrossRef]
218. Requena-Garcia-Cruz, M.V.; Cattari, S.; Bento, R.; Morales-Esteban, A. Comparative Study of Alternative Equivalent Frame Approaches for the Seismic Assessment of Masonry Buildings in OpenSees. *J. Build. Eng.* **2023**, *66*, 105877. [CrossRef]
219. Lagomarsino, S.; Cattari, S.; Angiolilli, M.; Bracchi, S.; Rota, M.; Penna, A. Modelling and Seismic Response Analysis of Existing URM Structures. Part 2: Archetypes of Italian Historical Buildings. *J. Earthq. Eng.* **2022**, *27*, 1849–1874. [CrossRef]
220. Jiménez-Pacheco, J.; González-Drigo, R.; Pujades Beneit, L.G.; Barbat, A.H.; Calderón-Brito, J. Traditional High-Rise Unreinforced Masonry Buildings: Modeling and Influence of Floor System Stiffening on Their Overall Seismic Response. *Int. J. Archit. Herit.* **2021**, *15*, 1547–1584. [CrossRef]
221. Belmouden, Y.; Lestuzzi, P. An Equivalent Frame Model for Seismic Analysis of Masonry and Reinforced Concrete Buildings. *Constr. Build. Mater.* **2009**, *23*, 40–53. [CrossRef]
222. Lagomarsino, S.; Penna, A.; Galasco, A.; Cattari, S. TREMURI Program: An Equivalent Frame Model for the Nonlinear Seismic Analysis of Masonry Buildings. *Eng. Struct.* **2013**, *56*, 1787–1799. [CrossRef]
223. Marques, R.; Lourenço, P.B. Unreinforced and Confined Masonry Buildings in Seismic Regions: Validation of Macro-Element Models and Cost Analysis. *Eng. Struct.* **2014**, *64*, 52–67. [CrossRef]
224. Cannizzaro, F.; Castellazzi, G.; Grillanda, N.; Pantò, B.; Petracca, M. Modelling the Nonlinear Static Response of a 2-Storey URM Benchmark Case Study: Comparison among Different Modelling Strategies Using Two- and Three-Dimensional Elements. *Bull. Earthq. Eng.* **2022**, *20*, 2085–2114. [CrossRef]
225. Betti, M.; Galano, L.; Vignoli, A. Time-History Seismic Analysis of Masonry Buildings: A Comparison between Two Non-Linear Modelling Approaches. *Buildings* **2015**, *5*, 597–621. [CrossRef]
226. Aşıkoğlu, A.; Vasconcelos, G.; Lourenço, P.B.; Pantò, B. Pushover Analysis of Unreinforced Irregular Masonry Buildings: Lessons from Different Modeling Approaches. *Eng. Struct.* **2020**, *218*, 110830. [CrossRef]
227. Dhanasekar, M.; Haider, W. Explicit Finite Element Analysis of Lightly Reinforced Masonry Shear Walls. *Comput. Struct.* **2008**, *86*, 15–26. [CrossRef]
228. Abdellatif, A.; Shedid, M.; Okail, H.; Abdelrahman, A. Numerical Modeling of Reinforced Masonry Walls under Lateral Loading at the Component Level Response as Opposed to System Level Response. *Ain Shams Eng. J.* **2019**, *10*, 435–451. [CrossRef]
229. Noor-E-Khuda, S.; Thambiratnam, D.P. In-Plane and out-of-Plane Structural Performance of Fully Grouted Reinforced Masonry Walls with Varying Reinforcement Ratio—A Numerical Study. *Eng. Struct.* **2021**, *248*, 113288. [CrossRef]
230. Li, J.; Weigel, T.A. Damage States for Reinforced CMU Masonry Shear Walls. In *Advances in Engineering Structures, Mechanics & Construction*; Solid Mechanics and Its Applications; Springer: Dordrecht, The Netherlands, 2006; Volume 140, pp. 111–120. [CrossRef]
231. FEMA. *Earthquake Loss Estimation Methodology HAZUS (1999)*; Federal Emergency Management Agency: Washington, DC, USA, 1999.
232. Murcia-Delso, J.; Shing, P.B. Fragility Analysis of Reinforced Masonry Shear Walls. *Earthq. Spectra* **2012**, *28*, 1523–1547. [CrossRef]
233. Porter, K.; Kennedy, R.; Bachman, R. Creating Fragility Functions for Performance-Based Earthquake Engineering. *Earthq. Spectra* **2007**, *23*, 471–489. [CrossRef]
234. Ruiz-García, J.; Negrete, M. Drift-Based Fragility Assessment of Confined Masonry Walls in Seismic Zones. *Eng. Struct.* **2009**, *31*, 170–181. [CrossRef]
235. Araya-Letelier, G.; Calderón, S.; Sandoval, C.; Sanhueza, M.; Murcia-Delso, J. Fragility Functions for Partially-Grouted Masonry Shear Walls with Bed-Joint Reinforcement. *Eng. Struct.* **2019**, *191*, 206–218. [CrossRef]
236. Lotfy, I.; Mohammadalizadeh, T.; Ahmadi, F.; Soroushian, S. Fragility Functions for Displacement-Based Seismic Design of Reinforced Masonry Wall Structures. *J. Earthq. Eng.* **2022**, *26*, 33–51. [CrossRef]
237. Rezaei, S.; Dolatshahi, K.M.; Asjodi, A.H. Multivariable Fragility Curves for Unreinforced Masonry Walls. *Bull. Earthq. Eng.* **2023**, *21*, 3357–3398. [CrossRef]
238. Asjodi, A.H.; Dolatshahi, K.M. Extended Fragility Surfaces for Unreinforced Masonry Walls Using Vision-Derived Damage Parameters. *Eng. Struct.* **2023**, *278*, 115467. [CrossRef]
239. Snoj, J.; Dolšek, M. Fragility Functions for Unreinforced Masonry Walls Made from Hollow Clay Units. *Eng. Struct.* **2017**, *145*, 293–304. [CrossRef]
240. Hamzeh, L.; Ashour, A.; Galal, K. Development of Fragility Curves for Reinforced-Masonry Structural Walls with Boundary Elements. *J. Perform. Constr. Facil.* **2018**, *32*, 04018034. [CrossRef]
241. Riahi, Z.; Elwood, K.J.; Alcocer, S.M. Backbone Model for Confined Masonry Walls for Performance-Based Seismic Design. *J. Struct. Eng.* **2009**, *135*, 644–654. [CrossRef]
242. Panchal, V.R.; Jangid, R.S. Seismic Response of Structures with Variable Friction Pendulum System. *J. Earthq. Eng.* **2009**, *13*, 193–216. [CrossRef]

243. Matsagar, V.A.; Jangid, R.S. Base Isolation for Seismic Retrofitting of Structures. *Pract. Period. Struct. Des. Constr.* **2008**, *13*, 175–185. [CrossRef]
244. Aghabeigi, P.; Farahmand-Tabar, S. Seismic Vulnerability Assessment and Retrofitting of Historic Masonry Building of Malek Timche in Tabriz Grand Bazaar. *Eng. Struct.* **2021**, *240*, 112418. [CrossRef]
245. Michel, C.; Karbassi, A.; Lestuzzi, P. Evaluation of the Seismic Retrofitting of an Unreinforced Masonry Building Using Numerical Modeling and Ambient Vibration Measurements. *Eng. Struct.* **2018**, *158*, 124–135. [CrossRef]
246. Karbassi, A.; Nollet, M.J. Performance-Based Seismic Vulnerability Evaluation of Masonry Buildings Using Applied Element Method in a Nonlinear Dynamic-Based Analytical Procedure. *Earthq. Spectra* **2013**, *29*, 399–426. [CrossRef]
247. Frankie, T.M.; Gencturk, B.; Elnashai, A.S. Simulation-Based Fragility Relationships for Unreinforced Masonry Buildings. *J. Struct. Eng.* **2013**, *139*, 400–410. [CrossRef]
248. Siyam, M.A.; Konstantinidis, D.; El-Dakhakhni, W. Collapse Fragility Evaluation of Ductile Reinforced Concrete Block Wall Systems for Seismic Risk Assessment. *J. Perform. Constr. Facil.* **2016**, *30*, 04016047. [CrossRef]
249. Derakhshan, H.; Walsh, K.Q.; Ingham, J.M.; Griffith, M.C.; Thambiratnam, D.P. Seismic Fragility Assessment of Nonstructural Components in Unreinforced Clay Brick Masonry Buildings. *Earthq. Eng. Struct. Dyn.* **2020**, *49*, 285–300. [CrossRef]
250. Giordano, N.; DeLuca, F.; Sextos, A. Analytical Fragility Curves for Masonry School Building Portfolios in Nepal. *Bull. Earthq. Eng.* **2021**, *19*, 1121–1150. [CrossRef]
251. Dong, Z.Q.; Li, G.; Song, B.; Lu, G.H.; Li, H.N. Failure Risk Assessment Method of Masonry Structures under Earthquakes and Flood Scouring. *Mech. Adv. Mater. Struct.* **2022**, *29*, 3055–3066. [CrossRef]
252. Losanno, D.; Ravichandran, N.; Parisi, F. Seismic Fragility Models for Base-Isolated Unreinforced Masonry Buildings with Fibre-Reinforced Elastomeric Isolators. *Earthq. Eng. Struct. Dyn.* **2023**, *52*, 308–334. [CrossRef]